DEVELOPMENT OF ACTIVE RESPONSE TECHNOLOGY FOR SAFETY APPLICATIONS IN POWER SAWS

BY

MARIN I. ASSALIYSKI

Submitted in partial fulfillment of the
requirements for the degree of
Master of Science in Mechanical and Aerospace Engineering
in the Graduate College of the
Illinois Institute of Technology

Approved _______________
Advisor

Chicago, Illinois
May 2014

ACKNOWLEDGMENT

I would like to sincerely and gratefully thank my advisor Dr. Matthew Spenko, as well as Jan Koegel and Bob Newton from the Robert Bosch Tool Corporation, for their guidance, encouragement, and patience along the way. I would also like to greatly thank my committee members, Dr. Boris Pervan and Dr. Francisco Ruiz, for their assistance.

Especially deep gratitude goes to my parents, Ivan and Mariyka Assaliyski, for believing in me and supporting me throughout my thesis work. Without their relentless encouragement this work would not have been possible, Thank You!

TABLE OF CONTENTS

LIST OF TABLES

LIST OF FIGURES

LIST OF SYMBOLS

Symbol	Definition
$\boldsymbol{\omega}$	Blade Angular Velocity (RPM=$\frac{revolutions}{minute}$)
$\boldsymbol{\alpha}$	Blade Angular Acceleration ($\frac{RPM}{sec}$)
Γ	Blade Angular Acceleration Detection Threshold ($\frac{RPM}{sec}$)
δ	Blade Thickness (mm)
ϵ	Kerf (Cut) Width (mm)
$\mathbf{F}$	Impact Force (N)
$\boldsymbol{x}$	Work piece distance (m)
$\dot{\boldsymbol{x}}$	Kickback Velocity of Workpiece ($\frac{m}{s}$)
$\ddot{\boldsymbol{x}}$	Kickback Acceleration of Workpiece ($\frac{m}{s^2}$)
F_S	Data acquisition sampling frequency (Hz)
$\boldsymbol{\zeta}$	State vector
$\mathbf{z}$	Measurement vector
$\mathbf{L_K}$	Kalman gain matrix
$\boldsymbol{\Phi}$	State transition matrix
$\bar{\mathbf{P}}$	Covariance at time update
$\hat{\mathbf{P}}$	Covariance at measurement update
$\bar{\boldsymbol{\zeta}}$	State vector at time update
$\hat{\boldsymbol{\zeta}}$	State vector at measurement update
$\boldsymbol{\Gamma}$	Input matrix
$\mathbf{H}$	State observation matrix
$\mathbf{W}$	Process noise covariance

$\mathbf{V}$	Observation noise covariance
$\boldsymbol{F}$	System matrix

ABSTRACT

This thesis presents a study of kickback occurrences on table saws, as well as the development and evaluation of a system designed to mitigate health and property hazards due to kickbacks. A kickback is an unwanted situation during the cutting process of many powered circular saw tools, during which the operator of the tool loses control, potentially resulting in severe property and bodily harm. Multiple safety devises exist to prevent this type of situation from occurring; however, all of these devices are passive and often become a burden by decreasing efficiency, and are therefore often removed by the users. This thesis seeks to study the occurrence of kickbacks and to present an active electronic detection system that is able to aid in mitigation of potential damage to property or persons by developing responsive, robust, and practical methods of kickback detection. Implemented detection methods are presented and evaluated for performance. Concepts are also developed, presented, and discussed with the purpose of generating topics for future work. An experimental brake is used to evaluate the performance of the detection methods with an integrated system.

CHAPTER 1
INTRODUCTION

Power tools have been a major enabling factor over the decades in allowing the construction of structures in an affordable, efficient and quick manner. A large portion of these power tools are saws which include table saws, portable circular saws, and miter saws (see Figures 1.6, 1.1, and 1.2 respectively). With the performance increase that they bring to a construction crew, they also bring inherent safety issues, which cannot be avoided. Even greater safety issues lie with use of these tools within the do-it-yourself (DIY) market. The safety issues addressed by this thesis apply to most power tools with rotating circular blades. All of these types of saws have experienced increased use across all markets; however, for the purpose of simplification and developing a robust understanding of the issues, and options for addressing them, the focus of this thesis will be limited to table saws.

Figure 1.1. Example of a circular saw

With an increase in use by professionals and by DIY users, there has been a substantial increase in personal injuries as well. This increase has caught the attention

Figure 1.2. Example of a miter saw

of government regulators and of the entire power tools industry. Since the 2000's, the United States government has been gathering and publishing information on the occurrences and reasons for injuries on a regular basis. In 2011, the U.S. Consumer Product Safety Commission (USCPSC) evaluated the various technologies available to address the dangers [Smi11]. The commission also carried out a survey of injuries in table and bench top saws in 2007 and 2008, which clearly shows the increase in frequency of such occurrences as well as the causes [CP11].

Although such injuries may be thought of as effecting only those directly involved, another report by the U.S. Consumer Product Safety Commission from 2003 [MRM03] clearly demonstrates how the large amount of injuries and the high long-term cost of these injuries translate into costs for the overall economy in ways that maybe be superficially unexpected. One of the categories of power tools with the highest "Estimated Cost Index" is bench or table saws, with a value of $1,967,000,000 within the range of 1997 to 2002, as illustrated in Figure 1.3. This is a staggering value which includes contributions from various expense sources; however, the most interesting finding in the report is that 96% of these costs are "addressable," which

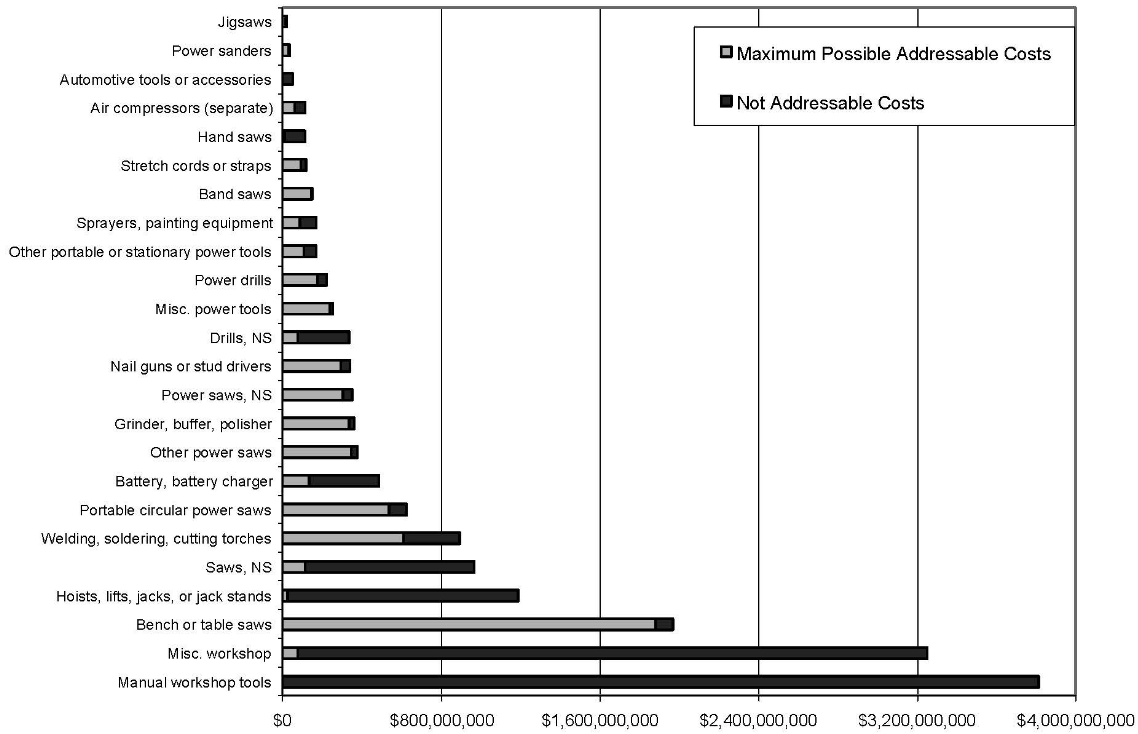

Figure 1.3. Estimated cost index for power equipment [MRM03].

is defined in the report as:

> The maximum addressable cost estimate does not necessarily represent the injury and death costs that the USCPSC might actually be able to prevent each year through some type of action. It represents only a target population from which any successful prevention will have to come.

Essentially, the figure represents areas of costs that are amenable to reduction by different means; however, it does not necessarily mean that all or even any significant portion can be prevented at this point. If nothing more, this value is a clear sign of the vast need for implementation of some type of safety devices or different means of using these tools in order to diminish unnecessary cost and most importantly unnecessary injuries.

Figures 1.4 and 1.5 are examples of minor injuries due to kickback. Many cases however can be quite severe, ranging from amputations to death [CP11].

Figure 1.4. Minor hand injury due to kickback [Spa12]

Therefore, the power tool industry has a high interest in developing safety products to alleviate these losses. A more subtle, yet just as significant motivator, is the factor of liability. As these reports are published, the loss of life and property is more evident. Combined with the reports evaluating the effectiveness of current safety methods and devices, one can possibly attempt to transfer liability from any incidents to the manufacturer of these tools. This is something that happens quite frequently and the best defense power tool manufacturers have is to actually put maximum efforts in developing technologies to safeguard users. Designing and manufacturing safe tools is already a top priority for every manufacturer; however, the vast amount of mechanisms by which persons can injure themselves can be challenging to address is a short amount of time. Development and implementation of safety systems takes especially long due to the need to provide robust and effective devices, otherwise providing “false-hope” safety devices will not beneficially serve anyone.

One of the largest power tool manufacturers in the world is Robert Bosch Tool

Figure 1.5. Abdominal injury due to kickback projectile [Jas10]

Corporation (BOSCH), with whose assistance the research and development in this thesis has been conducted. BOSCH is dedicating significant efforts to ensure that their tools are produced with the safety of the user as a top priority. BOSCH has been a leader in the development of personal protection devices and methods in power tools. Most recently, they introduced a novel blade guard that attempts to provide the user with maximum ease of use while still offering significant protection.

In this thesis a concentrated effort is made to address safety concerns due to kickback, a safety issue which has become a leading priority. This will be addressed by presenting relevant information from various sources, developing further details as to the causes and effects through experimentation, and practically implementing a mechatronic system to serve as a platform for developing and evaluating various methods of detection and mitigation.

1.1 Background

This thesis focuses on a table saw, specifically the Bosch GTS 10 XC as shown

Figure 1.6. Example of a table saw (Bosch GTS 10 XC)

in Figure 1.6. The tool is mainly sold in European markets with a high volume of sales. Thus, it is ideal for initial assessment. Although safety regulations vary between European and U.S. markets, the general safety mechanisms built into the tool are very similar, as are the performance specifications. Typically table saws are used to alter, technically referred to as ripping, the dimensions of long pieces of wood. This includes anything from structural wooden studs to flooring supports such as plywood, to fine finishing work such as cabinetry.

Table 1.1. Published motor specifications for the Bosch GTS 10 XC

Parameter	Specified Value
Power Rating	1650 Watts
Amp Rating	15 Amps
Voltage	110 VAC
Nominal Speed	$4,200\frac{Revolutions}{Minute}$
Convenience Braking Time	$\sim 2 - 3s$

Table saws have mechanisms for adjusting the height of the saw blade, allowing the user to vary it according to the thickness of the material being cut. Additionally most saws, such as the Bosch GTS 10 XC, have the ability or bevel the blade, allowing the user to make angled cuts relative to the saw table top. This requires the tool to be very versatile in the type of material it can cut as well as the quality of cut that it produces. These requirements mainly influence the motor parameters of torque and saw blade speed. To allow for versatility and performance, they are typically designed with powerful motors that run at high speeds. Typical specifications for the Bosch GTS 10 XC are noted in Table 1.1.

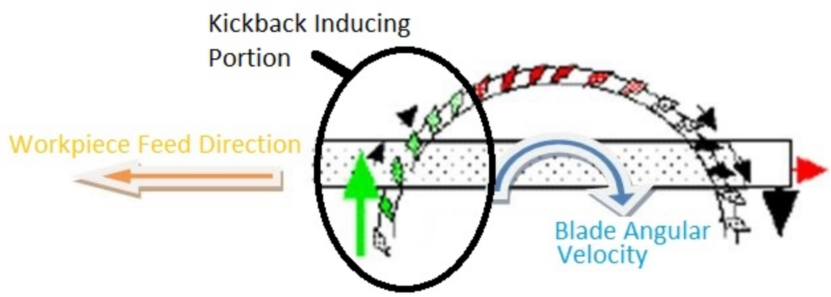

Figure 1.7. Influence of blade areas on kickback

In the most general sense, a kickback is induced whenever there is a significant interaction between the blade and the teeth at the back of the blade, in Figure 1.7 this portion is circled and noted. The issue is that, if for any reason the kerf closes up or becomes misaligned from being parallel to the blade, friction will being to build up and since the velocity vector of the teeth at this location generally point in the vertical direction, then the work piece will be lifted off the work table. In itself this is not a critical problem, but once the work piece is off the table, it will begin to make contact with the teeth at the top of the blade. At this point the main issue arises; the velocity vector of the teeth at the top is directed opposite to the feed direction. Depending on the amount of binding and friction that is developed, there can and usually is a rapid and significant transfer of energy from the blade to the work piece, giving it velocity opposite the feed direction, which builds up abruptly in a manner of 100 to 200 milliseconds.

Due to the power of the motor, kickback and other safety issues can cause significant damages. In the following paragraphs, the current leading safety devices are discussed.

Figure 1.8. Table saw blade guard

The first, and most critical, line of defence is the blade guard as shown in Figure 1.8. The main function of the guard is to serve as a physical barrier between the saw blade and the user. The blade guard is not a trivial device, as it must perform its function without hindering the use of the tool. Since the inception of the table saw, manufacturers have gone through many iterations to reach the design shown in Figure 1.8. As mentioned, the blade guard must provide its safety functions while allowing for the ease of use required by the operator. This includes allowing maximum visibility of the cutting process, allowing for the proper means of dust removal, as well as being easy to remove. For this reason, the shown blade guard is a two piece design, which allows it to easily ride to top of uneven work pieces and provide maximum protection even when the saw blade is beveled relative to the table top. The two piece design also satisfies user's requirement to have clear line of sight to the cutting location. The device is a major advancement in safety, mainly for the reason that it is unobtrusive to the user, relative to previous designs. This factor is essential, because as detailed by the USCPSC, many table saw operators remove the blade guards from their tools because they do not allow them to effectively use the tool [Smi11]. As will become evident, this is a major issue with all of the passive safety devices described in this chapter, and is the leading cause for the need to developed active safety systems that do not need to be removed, and cannot be removed, by the user.

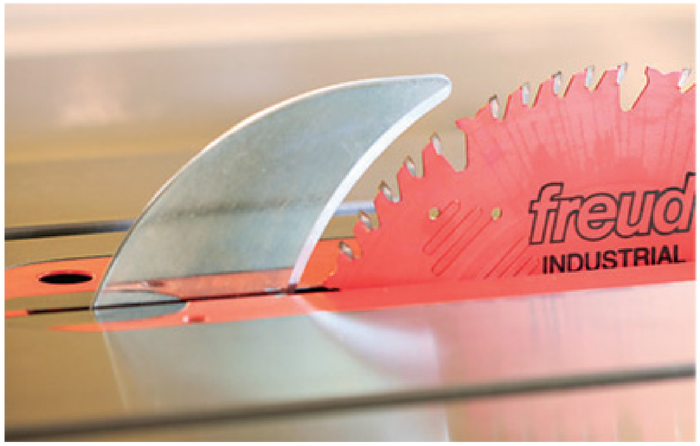

Figure 1.9. Table saw riving knife

Another common safety device is called a riving knife, as shown in Figure 1.9. This is essentially a thin, flat piece of metal which sits directly behind the saw blade, such that it passes through the kerf, or cut left by the blade, as the work piece is fed through the tool. The main function of the riving knife is to prevent the kerf from closing up or for the entire workpiece to shift from parallel with respect to the saw blade. This is the main line of defense against kickback with passive devices, and performs very well when properly installed. The means of protection by the riving knife from kickbacks is described further below. Additionally, the riving knife serves as the attachment point for the blade guard, and the anti-kickback paws which are described below. Unfortunately, the issues with the riving knife surrounds the fact that it is a passive device that can be in the way during certain legitimate cutting operations and is thus often removed. Similar to the blade guard, when the riving knife is removed, the user often neglects to replace it. Not replacing the riving knife leaves the tool very vulnerable to kickbacks while simultaneously leaving the blade exposed since the baled guard cannot be installed without it. Aside from removing and failing to replace the riving knife, other potential issues may arise if it is not properly aligned. Since the thickness of the riving knife is only slightly thinner than the actual thickness of the blade, even small misalignments can cause work piece jamming issues. Sometimes even the misaligned riving knife can by itself induce a kickback. Again the need for an active safety system is evident, one which can be active at all times without being intrusive.

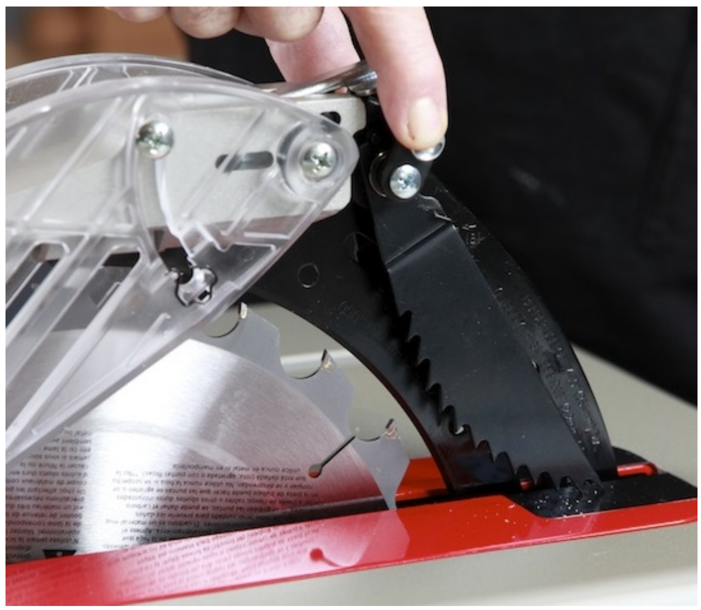

Figure 1.10. Table saw anti-kickback paws

An additional safety device, having the sole purpose of preventing kickbacks, are the anti-kickback paws as shown in Figure 1.10. The anti-kickback paws attach to the back side of the riving knife, where during normal feeding of the work piece through the tool they glide above it, with minimal downward force provided by tension springs. The teeth on the paws are oriented such that if a kickback occurs and the work-piece begins to move in the opposite direction to feeding, the slight tension from the springs will cause the teeth to dig into the work-piece and prevent it from moving. This is also an effective device when installed properly. As with the blade guard, if the riving knife is removed, the kickback paws cannot be used. The paws do add an amount of inconvenience to the user, in that they may prevent legitimate attempts for the user to pull back the work piece for whatever reason. The tension provided by the springs can provide an additional drawback to this device by causing the paws to damage delicate materials by scraping the surface.

Figure 1.11. Table saw rip fence

The final safety device described here is the rip fence, typically an extrusion running from the front of the table top to the back aligned parallel to the saw blade, as shown in Figure 1.11. The rip fence serves to align and guide the work piece as it is being fed through the tool. It mainly functions to provide a clean and straight cut; however, keeping the line of cut straight is also very important in preventing a kickback from occurring as well as from jamming the saw blade. The rip fence slides along the table top to allow for various widths of work pieces to be cut, and it can also be easily removed to cut very large pieces. Cutting without a rip fence is quite dangerous. Without it, this task becomes more difficult and the likelihood of a kickback occurring increases substantially.

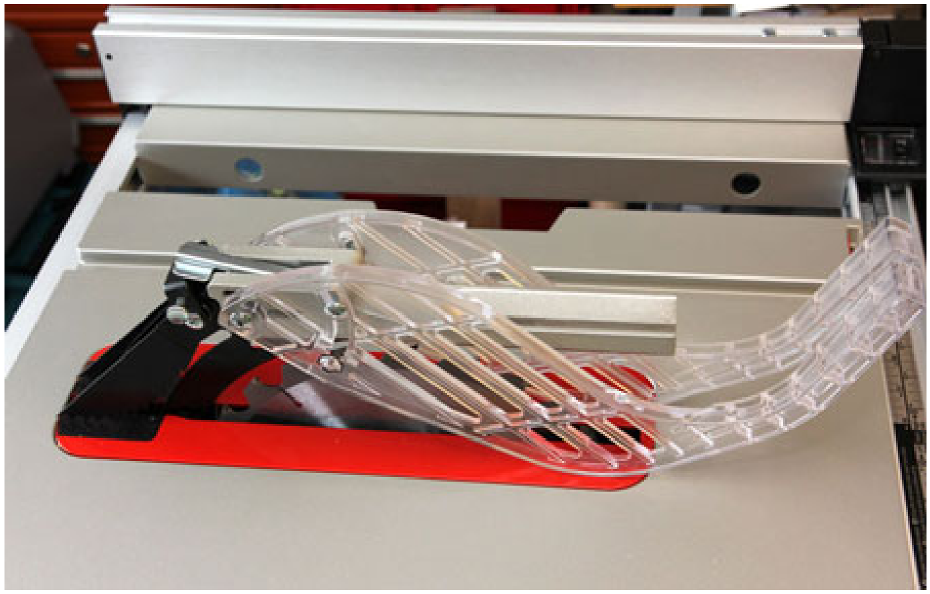

Figure 1.12. Assembly of safety devices typically standard on table saws

The four passive safety devices discussed above are the standard protection available to the user in terms of preventing contact with the saw blade or preventing kickback. These devices are very effective when installed and aligned properly; however, a substantial amount of users tend to remove them for various reasons, or simply have not aligned them properly. Through the life of the tool it is inevitable that for various reason components such as the riving knife and the rip fence may become misaligned relative to the saw blade. Often neglected by users, this is a significant cause of kickbacks [Smi11]. The complete assembly of these devices is illustrated in Figure 1.12. By reviewing the current leading safety devices, it is clear why there is an industry trend to developed more advanced active sensing and mitigation methods which can assist in the prevention of injury, alongside, or in replacement of some of the passive devices.

Figure 1.13 shows an annotated representation of the involved components on a table saw during a cutting process and potential kickback. In this figure, areas indicated by arrows have a positive correlation to a kickback occurrence.

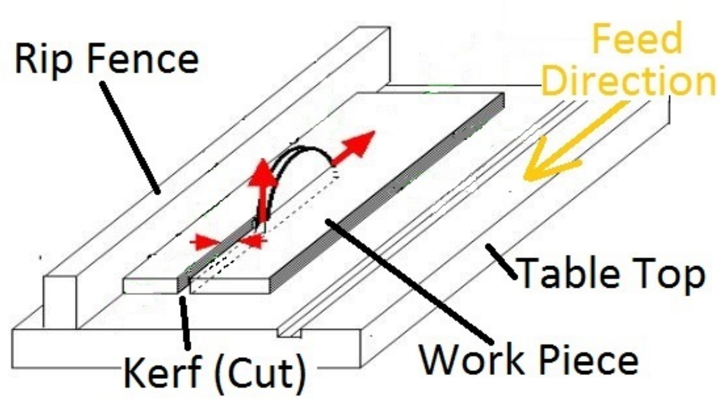

Figure 1.13. Forces contributing to kickback occurrence

To address the task of preventing or mitigating a kickback event, a certain level of understanding of the process is necessary. Due to the high number of variables involved, many of which there is no way to control, the use of standard research approaches is limited. For instance, an initial interest for this thesis was to develop a dynamic model of cutting process which would incorporate provisions for occurrences of a kickback event, such that the model can be compared to data from sensors in real time and deviations can be detected. As study of the event progressed, it became evident that it is nearly impossible, and extremely impractical, to develop such a model due to the high number of uncontrollable variables, for many of which no sensor could be practically and cost effectively employed to provide data. For this reason it was decided to take an empirical approach and develop at most highly simplified models of the tool/cutting process which could be used to detect deviations from normal operation. The details of the involved variables and simplifications employed as part of the study are presented in Chapter 2.

1.2 Summary of Contributions

The contributions of this thesis are:

- Study and statistical parametrization of kickback events to build on previously available information [Bel02].

- Development of functional requirements for kickback detection and mitigation systems with a focus on the severity of bodily damage [SCB+12].
- Implementation of a real-time mechatronic system for kickback study, which additionally serves as a practical development platform for detection methods.
- Implementation and experimental performance evaluation of detection methods based on saw-blade speed and tool vibration data.

CHAPTER 2
KICKBACK STUDY AND ANALYSIS

Due to the lack of readily available data on how a kickback event occurs, as well as the transient effects of it, the first part of this thesis focuses on experimentally collecting data from induced/simulated kickbacks. This data is used to develop an understanding of how a kickback event unfolds, determine how sensitive the severity of the kickback is to the controlled variables, and to demonstrate the practicality of detection methods based on the applied sensing methods.

The main goal is to collect enough data of kickback events such that a robust statistical understanding can be developed. Understanding properties such as the overall duration of a kickback τ, the projectile velocities $\boldsymbol{v}$, and the potential impact force $\mathbf{F}$ are all necessary to develop an understanding of the health hazards potential and to design a system that can effectively diminish this effect.

Part of this study also seeks to identify any possible kickback patterns in the collected data so that detection methods can be developed as given in Section 2.3. Additionally, to understand which factors affect the severity of a kickback, the experimental setup is such that it allows for variation of a few key parameters. A challenge with this goal is that there are many variables involved during a kickback event, as noted in Table 2.1. Therefore, only variables that can practically be controlled will be evaluated.

Last, the experimental setup for the data collection is set up such that it can also serve as a demonstration of the technology that can be implemented in a product. Therefore all sensors that are used for the data collection process are acquired based on their performance and cost effectiveness. Likewise, a minimally modified production tool has been used for this experimental setup.

The software architecture, and its development process, can be envisioned as divided is phases. This serves to describe the flow of detection and mitigation, as well as the overall approach taken to the development of the project (see Figure 2.1). The first phase, sensing, deals with establishing a robust platform for acquiring and pre-processing the data available through sensors. This includes the implementation of sensor data reading, and any required filtering and augmentation required to be able to properly utilize the information. Work on this phase is further discussed in Subsection 2.1.2. Following is the processing phase, where algorithms for detection and evaluation for the need of mitigation is performed. A large portion of this thesis deals with developing, implementing, and evaluating the performance of detection methods, as discussed in Section 2.3. The final phase, mitigation or actuation, is where the physical interaction occurs. In this phase, various braking methods can be employed to satisfy the overall system requirements. The focus of this project is not on developing braking technology; however, the analysis and development of braking requirements is performed in the following sections. Additionally, a combined experimental test platform is described in Chapter 3 and is used to evaluate the overall system performance.

Figure 2.1. Project phases

The following section will detail the data of interest and how it was collected. In further sections, the data is analyzed to extract any meaningful information, which is used to develop the system functional requirements.

2.1 Experimental Setup

A major challenge in studying kickback is the large number of variables involved in the physical system. In order to set up an effective and insightful experimental procedure, the variables involved need to be identified and controlled as much as possible. As identified, the variables are shown in Table 2.1, along with comments on whether they are controllable for the purpose of these experiments, and whether they are varied through the trials to look for any correlation with the occurrence and severity of kickbacks.

Table 2.1. Experimental setup variables

Variables	Was Varied?	Was Controlled?
Tool Properties		
Blade Height	No	Yes
Blade Angle	No	Yes
Blade Properties	Yes	Yes
Number of teeth		
Tooth geometry		
Motor Properties	No	Yes
Nominal speed		
Nominal power		
Operating torque range		
Work-piece Properties		
Material	Yes	Yes
Cut Path Properties	Yes	No
Dimensions (thickness)	Yes	Yes
Operational Properties		
Feed Rate	Yes	No
Feed Method	Yes	Yes

In light of these constraints, we expect that focusing on the vibrations of the tool, as well as the speed of the blade, will yield favorable results. Vibration data can be easily and affordably collected by accelerometers. In this particular implementation, Micro-electromechanical Systems (MEMS) accelerometers are used. A notable issue, which is addressed in the following sections, is the poor performance of MEMS accelerometers for vibration measurements. The issue lies with susceptibility to a shifting of the DC bias while subjected to high energy, high frequency vibrations.

Since the speed of the rotating blade will be directly impacted by any binding, or irregular contact with the work piece, focus will be placed on acquiring the rotation speed of the blade as well.

An additional focus for the experimental data collection is the movement of the work piece. In order to obtain the data required to understand the statistics of kickback events, it is necessary to collect detailed information on the work piece being cut. Basic information such as mass and dimensions is recorded; however, in this case the velocity and acceleration of the work piece are critical. For this purpose a draw wire sensor containing a potentiometer is used to measure the work piece position. This allows for the distance between the sensor and the work piece, $\mathbf{x}$, to be tracked at all times. This data is derived to yield the velocity, $\dot{\mathbf{x}}$, and acceleration of the work piece, $\ddot{\mathbf{x}}$. Table 2.2 summarizes the sensing elements and the data associated.

Table 2.2. Data acquisition sensors

Sensor	Acquired Data
Quadrature Angular Encoder	Angular velocity of tool blade ω
3-Axis MEMS Accelerometer	Vibration data in 3-axis
Draw Wire Potentiometer	Test piece distance measurement x

2.1.1 Table Saw Kickback Setup. A considerable challenge was encountered when defining the experimental setup of the table saw. The setup had to be sufficient to collect data for normal cutting operations as well as data from kickback events. An alternative to collecting data from natural kickback events is to induce kickback via several different methods.

From initial information about kickbacks [Bel02], one of the most common ways that a kickback occurs is when ripping (i.e. cutting a piece of wood lengthwise) a long work piece without a rip fence, which makes it very likely that the line of cut will not be straight and binding between the cut edges and the saw blade will occur. When this happens, a kickback event is highly likely. However, safety issues arise when attempting to do this for the purpose of simulating a kickback, mainly that the person responsible for feeding the piece of wood into the saw is in a position in the line of a potential kickback. Feeding the work piece from the back is not possible, and a two person feeding operation increases the potential for errors and someone being injured.

For this reason any manual feeding is required it must be done from the side of the tool. To accomplish this, a setup was chosen such that the work piece is fed in manually by an operator standing to the side of the tool, while the work piece is guided along a slot in the saws table top. At a certain predefined point, a pneumatically actuated cylinder is triggered which binds the work piece with the blade causing the rear teeth of the blade to engage the work piece and induce the kickback. As soon as the piece of wood reaches the predefined point, the operator feeding in the work piece pulls back and allows the kickback to carry through. An overview of the layout of the experimental setup is shown in Figure 2.3.

This has been the most successful method for inducing a kickback from the various alternatives that were attempted. It does have a significant drawback however. The feed rate of the work piece into the tool cannot be controlled, even by

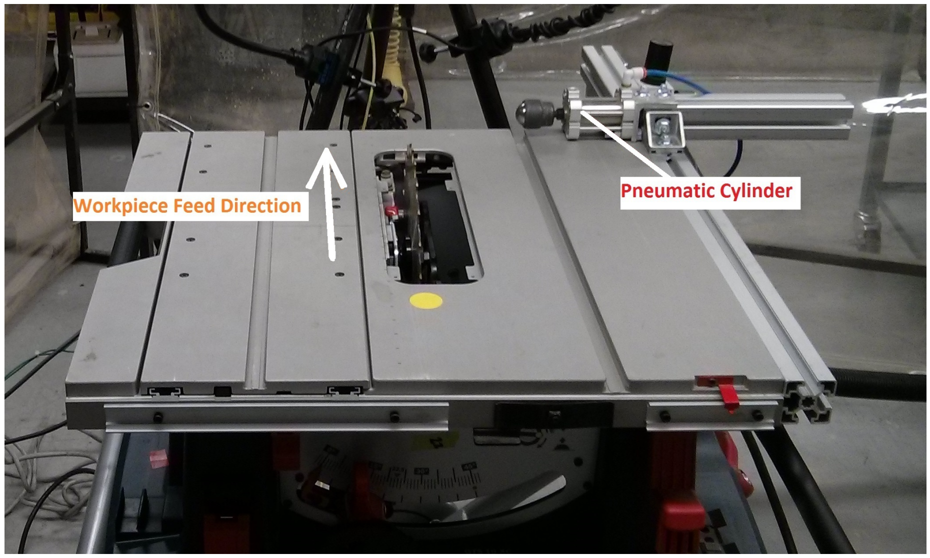

Figure 2.2. Close-up of saw table top and pneumatic cylinder

an experienced operator. An initial attempt involved a fully automated feeding and triggering mechanism, akin to a sled onto which the work piece would ride on and be fed into the saw. The major advantage of this was that the feed rate can be precisely controlled; however, the sled setup interfered with the progression of the kickback event.

Although feed rate is a major variable in the resulting kickback likelihood and severity, we decided that more useful data would be collected with an uncontrolled feed rate rather than a setup which did not allow for the full progression of the kickback event once it had been induced.

Figure 2.3 shows a picture of the overall setup used during kickback simulation. The tool used for the trials is the United Kingdom version of the Bosch GTS 10 XC (110 V) with no modifications to the drive train, and only minor modifications to the body in order to attach the sensors and pneumatic actuator. Various components of the setup as identified in Figure 2.3 are discussed subsequently.

The purpose of the draw wire sensor as shown in Figure 2.3 is to record the

Figure 2.3. Image showing the overall experimental setup

position of the work piece as the kickback occurs. Additionally, the position information from this sensor is used during the kickback simulation to trigger the kickback actuation cylinder at the precise predefined moment. This allows for increased control over the kickback setup, which is essential for the safety of the operators. The draw wire sensor used is produced by UniMeasure Inc. (Model: JX-PA-80-N12-21R-322) which is essentially a wire wound around a spring tensioned spool attached to a precise potentiometer. The end of the wire has a loop that attaches to a screw on the center of mass of the work piece.

The high speed camera (see Figure 2.3) is used to validate the collected data and better understand the sequence of events that transpire during kickback. All trials are recorded at a frame rate of 3,000 frames per second.

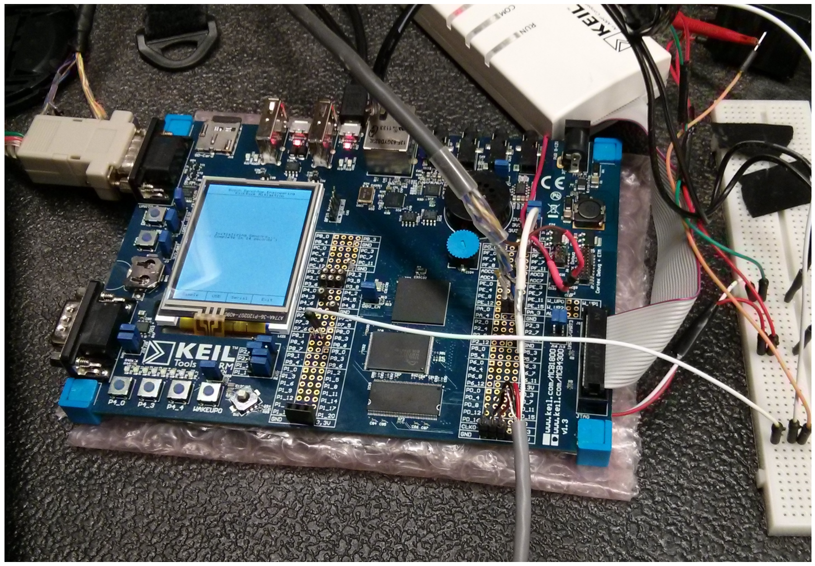

Figure 2.4. Experimental setup controller

Within the table saw are embedded the two primary sensors for data collection, which will be evaluated for possible use in kickback detection. These are the Quadrature Angular Encoder and the 3-Axis MEMS accelerometer. The position and attachment of these is shown in Figures 2.5 and 2.6 respectively.

As shown in Figure 2.5 the quadrature encoder is attached directly to the back end of the spinning motor armature via a coupling which has been tapped into the armature shaft. This position was chosen, as opposed to the output shaft of the drive-train due to the lower amount of mechanical noise (higher angular velocity stabilizes the armature better) as well as the higher resolution offered by the high angular velocity of the armature (about 22,000 RPM at armature versus about 3,800 RPM at output shaft). The encoder used is a 1,000 pulse per revolution (PPR) type, which provides 2,000 sense points per revolution when employing rising and falling edge pulse detection. The resolution, in revolutions per minute, provided by this implementation is about 5 RPM around the nominal idle speed of 3,800 RPM.

The accelerometer as shown in Figure 2.6 has the purpose of collecting vibra-

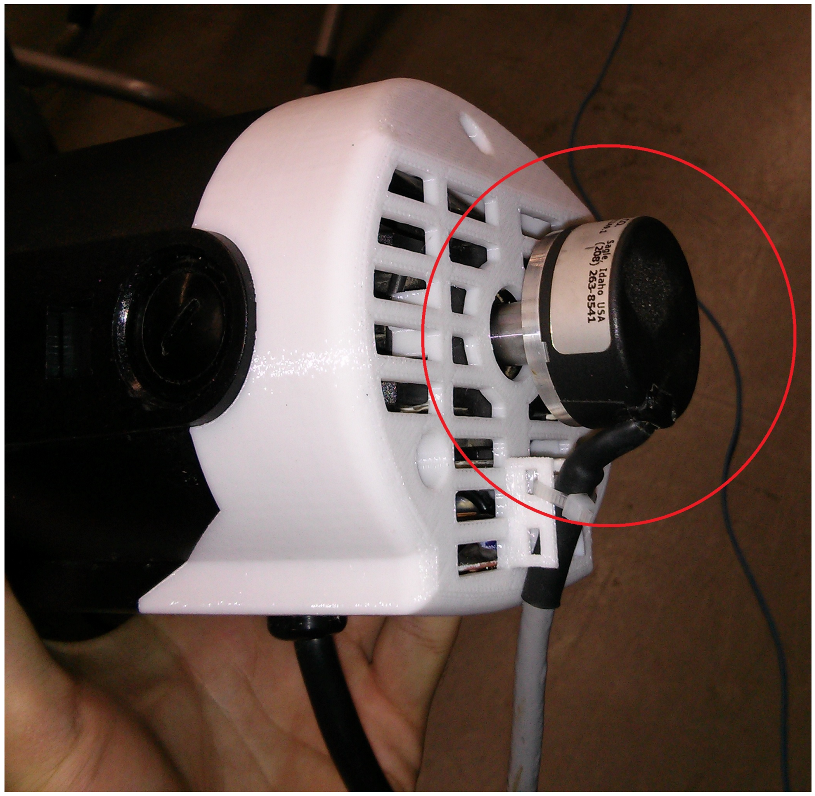

Figure 2.5. Angular velocity encoder attachment

tion data associated with the tool and any events transpiring, such as a kickback event. The hypothesis of employing an accelerometer is that it would give early warning through changes in the tools vibration signature that kickback is occuring. A MEMS accelerometer is not ideal for vibration data, since it is susceptible to DC offset; however, through verification with an AC IPC accelerometer we verified that with minimal or no filtering of low frequency vibrations, the frequency component of the data is accurate to within $\pm 5Hz$, which for the purpose of this project is adequate. Switching to an IPC accelerometer for much more accurate vibration data introduces a component of cost that would not be possible to implement in any type of production system. Therefore, it was decided that the MEMS accelerometer offer enough performance for the research phase as well as any upcoming production phases. In particular, the accelerometer implemented in this setup is the Bosch Sen-

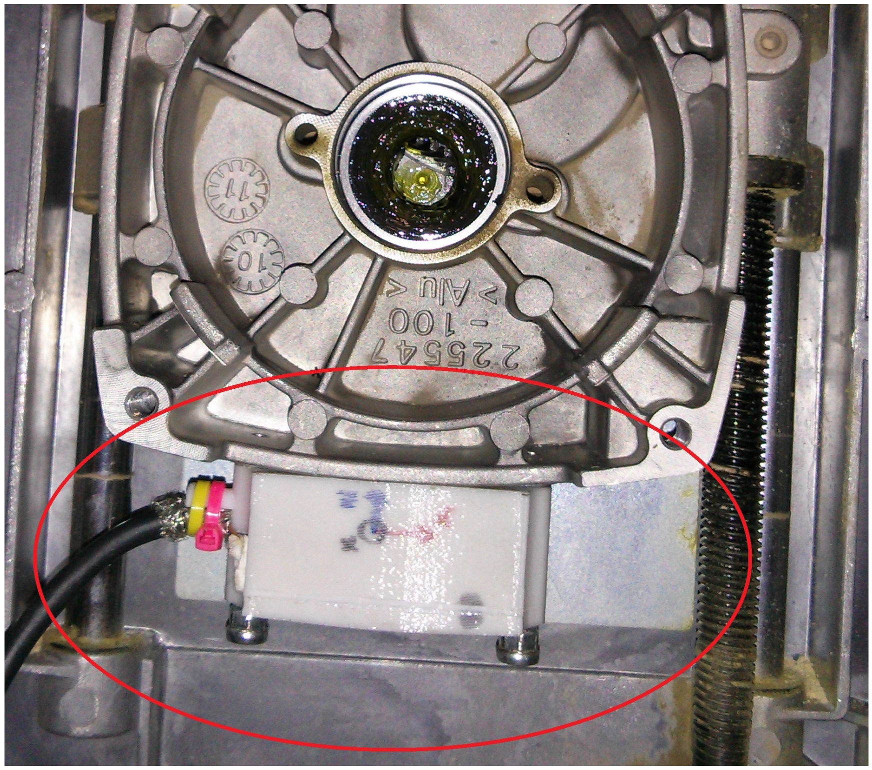

Figure 2.6. Accelerometer mounting

sorTec BMA255 model which offers excellent resolution and signal to noise ratio for the purpose of this project. Filtering details are discussed in Subsection 2.1.2.

2.1.2 Data Acquisition Hardware and Software. A custom purpose developed Data Acquisition (DAQ) System was developed to collect the data. As stated previously, this experimental setup is to also serve as a demonstration of a practical and cost effective detection/mitigation system, therefore commercial DAQ units were not employed due to cost. The DAQ has been developed in conjunction with the data collection effort, and has been revised multiples of times to meet the system requirements. The process taken has been iterative, with new information from previously collected data driving the direction of the DAQ hardware and software development. For instance, from previous knowledge that a kickback event has a duration of several hundred milliseconds, the initial DAQ was developed to sample at a frequency (F_S) of

100 Hz (10 milliseconds sampling interval). The collected data proved that the event was occurring much faster than previously expected, thus driving the development of the DAQ. This process was iterated with the sampling frequency as well as other DAQ parameters until the data collected was satisfactory in accurately representing the kickback event.

It is important to note that the data collected while fine tuning the DAQ to the application is not used for the actual analysis in the following sections. Separate data sets were collected to be used for analysis, with the interest of consistency and accuracy.

After initial assessment of the likely hardware requirements, in terms of computation, we decided to use the NXP LPC4357FET256 (LPC4357) micro-controller. This particular micro-controller was chosen due to its high performance processor and the wide range on-chip peripherals/functions that it offers (see Figure 2.7). This micro-controller contains two independent processing cores, but the second core was not used. Additionally, the processing cores are 32-bit wide and feature a high performance floating point unit (FPU), allowing it to evaluate non-integer calculations very fast and with high accuracy. Further, a highly attractive feature is the price of the processor, which for high volume orders is $8.64. It will be shown that this micro-controller is far more powerful than is required with the implementation described in this thesis; meaning that the cost of the micro-controller can further be reduced by implementing the software on a cheaper microchip for production. Table 2.3 provides the compete specifications of the micro-controller.

The LPC4357 is also a great choice for the application because it offers many useful on-chip peripherals that ultimately reduce the amount of additional external components required to complete the task. Figure 2.7 shows the block diagram of the micro-controller, where the used features are indicated by a thick box border.

Table 2.3. Micro-controller (NXP LPC4357FET256) specifications

Feature	Specification
Core processor	ARM Cortex M4/M0
Core size	32-Bit Dual-Core
Clock frequency (maximum)	180 (204) MHz
Program memory size (on-chip)	1 MB FLASH
EEPROM size	16 K x 8
RAM size	136 K x 8
Number of inputs/outputs	164
Data converters	A/D 8x10bit — D/A 1x10bit

A few of the most useful peripherals are the Quadrature Encoder Interface (QEI), Serial Peripheral Interface (SPI), Inter-Integrated Circuit (I2C), and the External Memory Controller (EMC).

The QEI peripheral is especially useful since the experimental setup uses a quadrature encoder to sense the angular velocity of the saw blade. This peripheral takes on a great deal of processing which would otherwise have to be performed by the processing core. The signal from the encoder arrives in the form of pulses over two separate channels, each channel offset from the other by 90 degrees, thus forming a quadrature signal that allows the direction and speed to be determined. This means that these pulses have to be continuously counted per an allotted time interval to determine the speed and direction. At full motor speed this requires lots of attention, which would interfere with more critical tasks to be processed by the core if the QEI were not available.

The SPI and I2C peripherals are data links which allow the micro-controller to exchange data with other processors, sensors, and other on-board devices. In this application, the SPI peripheral is used to exchange data with the accelerometer, as

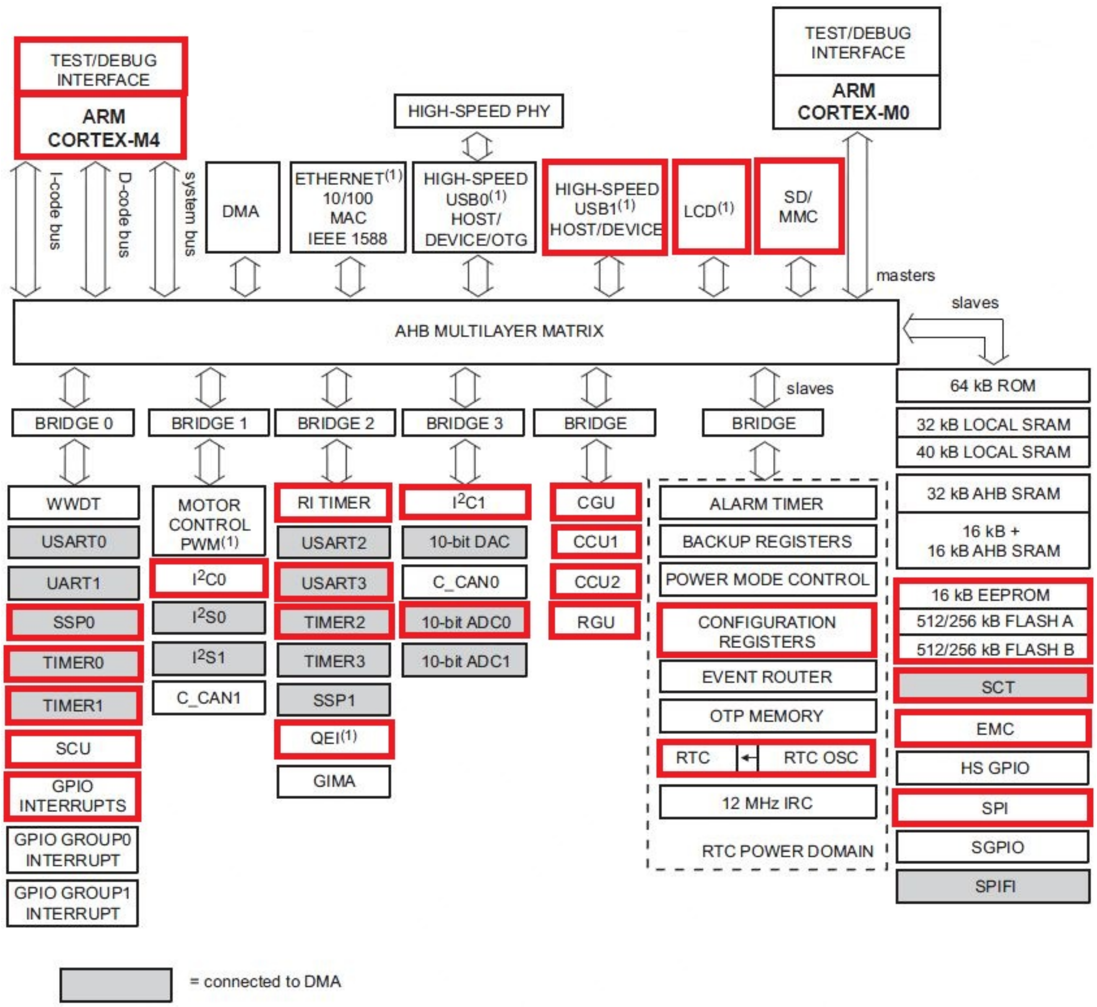

Figure 2.7. Block diagram of micro-controller (NXP LPC4357FET256)

well as to read and write data to the removable memory card. The I2C peripheral was implemented to control an external input/output extender.

The EMC was highly useful in this implementation because it allows for a high speed parallel 32-bit wide connection to external on-board memory, which is absolutely necessary in order to be able to save all of the acquired sensor data, as well as the computed data, fast enough to meet the sampling frequency requirements. Writing the data directly to the removable memory card over the SPI interface is not fast enough, therefore the data after each sampling interval is temporarily stored into the external Synchronous Dynamic Random Access Memory (SDRAM) chip until all samples are collected. After sampling has completed, the data is copied from SDRAM to permanent storage onto the removable memory card. Alternatively, high speed data can be saved onto the on-chip FLASH memory; however, in this application the amount of data per sample, combined with the total number of samples, is too large to be stored in the available 1MB capacity. For the purpose of illustrating the amount of data generated, sampling for 40 seconds at a frequency of 1 kHz produces 40,000 samples resulting in a little over 6 MB of data.

The remaining peripherals used are listed in Table 2.4 and reflect those indicated in Figure 2.7.

Table 2.4. Description of used micro-controller peripherals/registers

Peripheral/Register	Description
Clock Generation Unit (CGU)	Clock and power management
Clock Control Unit (CCU)	Clock selection for peripherals
System Control Unit (SCU)	Input/output pin configuration
Synchronous Serial Peripheral(SSP)	SPI Implementation
Real Time Clock (RTC)	Time-stamping log files
Repetitive Interrupt (RI) Timer	Sampling timer

The software used with this hardware has been developed as part of this thesis work and is optimized specifically for the application. Key requirements and features incorporated into the software are hard real-time execution and processing efficiency. Figure 2.8 shows a high level representation of the software architecture.

The most important requirement for the software is the ability to execute all code in a deterministic fashion. This is needed to ensure that all required functions, including data acquisition and evaluating detection methods, are completed before it is time to perform another sampling iteration. This is accomplished by a combination of powerful hardware and efficient application-specific software.

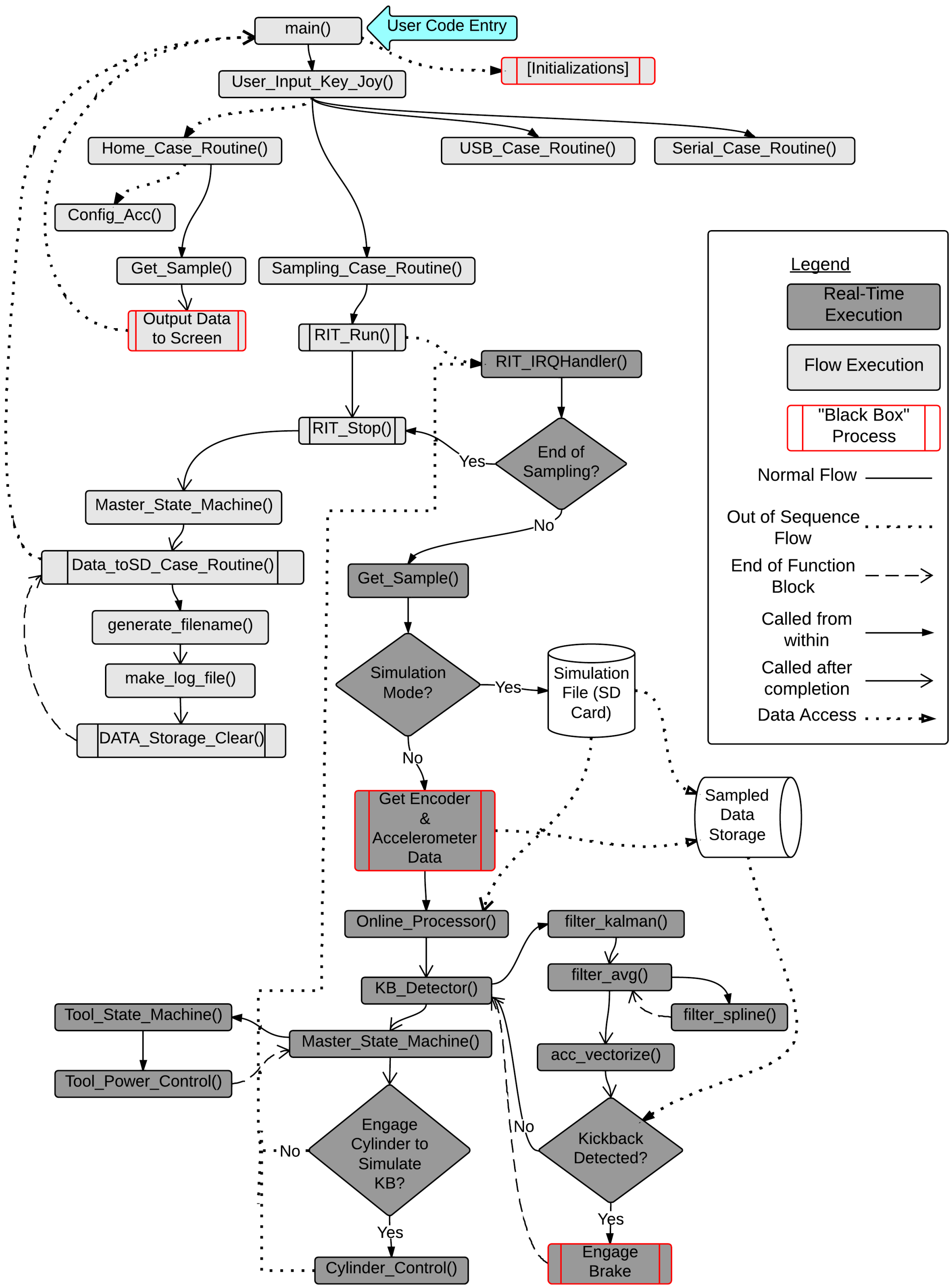

Figure 2.8. Software flow structure

The flow chart shown in Figure 2.8 shows the structure of the software. Not all code is executed in hard real-time, only the functions that require it. Blocks which are shaded dark in Figure 2.8 indicate a function executed in hard real-time, while light shading indicates executions that are not deterministic, and can vary from one cycle to the next. Essentially the functions indicated as running in real-time are those that are required during the sampling process. The rest are functions required for support tasks such as setup and user interface.

The efficiency of the implementation becomes evident when considering that the sampling frequency can be as high as 5 kHz, while performing all necessary data acquisition, pre-processing, Fast Fourier Transform (FFT) of size 128 samples, and evaluation against the detection methods. The sampling rate can be increased even further if computationally intensive tasks such as the FFT are not needed. To illustrate the stability of the deterministic timing, one of the timer peripherals was used to record how long each real-time processing cycle lasts, this is shown in Figure 2.9. This plot is equivalent to a processing load plot, since 1 millisecond is the available processor time and the average execution time is 0.2 milliseconds, then this means that the processor is operating at 20% load through the majority of a data acquisition trial.

In terms of a user interface, the DAQ has been developed to allow very simple one-button sampling initiation, as well as an interface allowing the modification of many system parameters while the DAQ is online. This is performed over a serial interface using the on-chip Universal Asynchronous Receiver/Transmitter (UART) peripheral. Using a serial-to-USB converter allows the DAQ system to be connected to any computer and controlled via command line. This is an example of part of the code which is executed in non real-time.

An important software feature implemented as part of the pre-processing of the

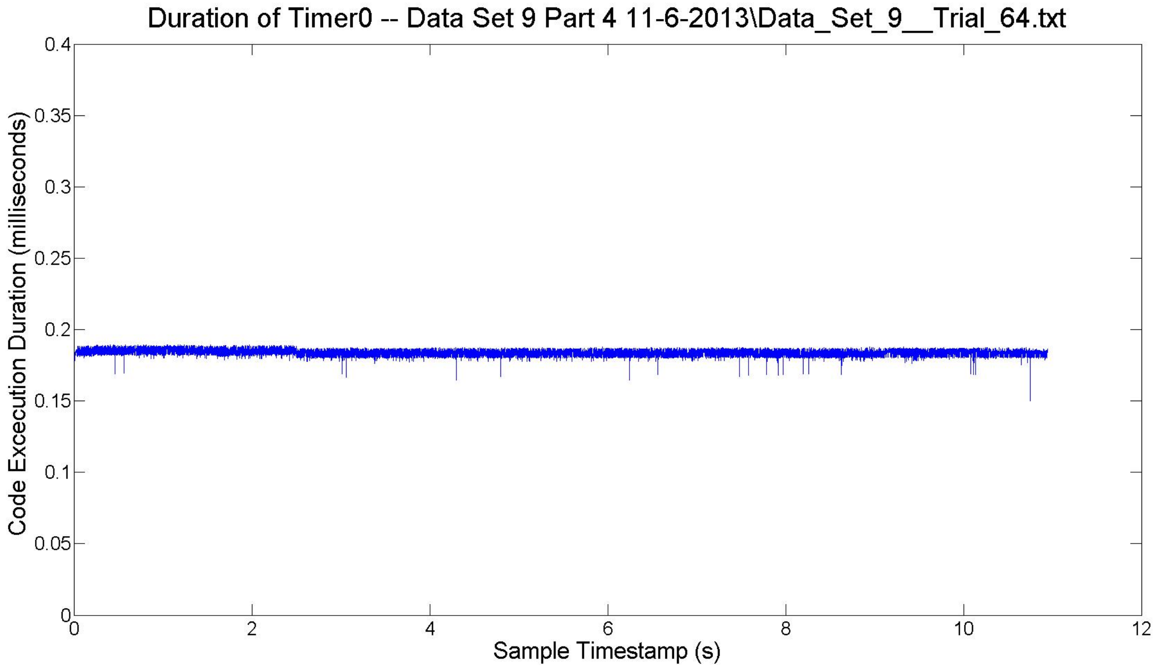

Figure 2.9. Execution duration of real-time processes per sample

acquired sensor data is the Kalman filter, additionally referred to as Linear Quadratic Estimation (LQE) [SHV12]. The Kalman filter is an ideal application in this case because it offers excellent performance with very light computational requirements. An additional advantage of using this filter is its ability to continuously adapt its gain setting according to the quality of the signal, which offers excellent performance with minimal knowledge of plant/process parameters. As applied here, it is used to significantly reduce noise from the encoder, accelerometer, and draw wire distance measurements. The details of the kalman filter implementation are shown in Appendix A

Figure 2.10 illustrates the performance of the filter by overlaying the raw data from the accelerometer with the one produced by the Kalman filter.

The successful incorporation of the Kalman filter proved to be an essential component in enabling the use of threshold methods, such as acceleration based detection, by suppressing noise and ultimately allowing fast detection and minimizing

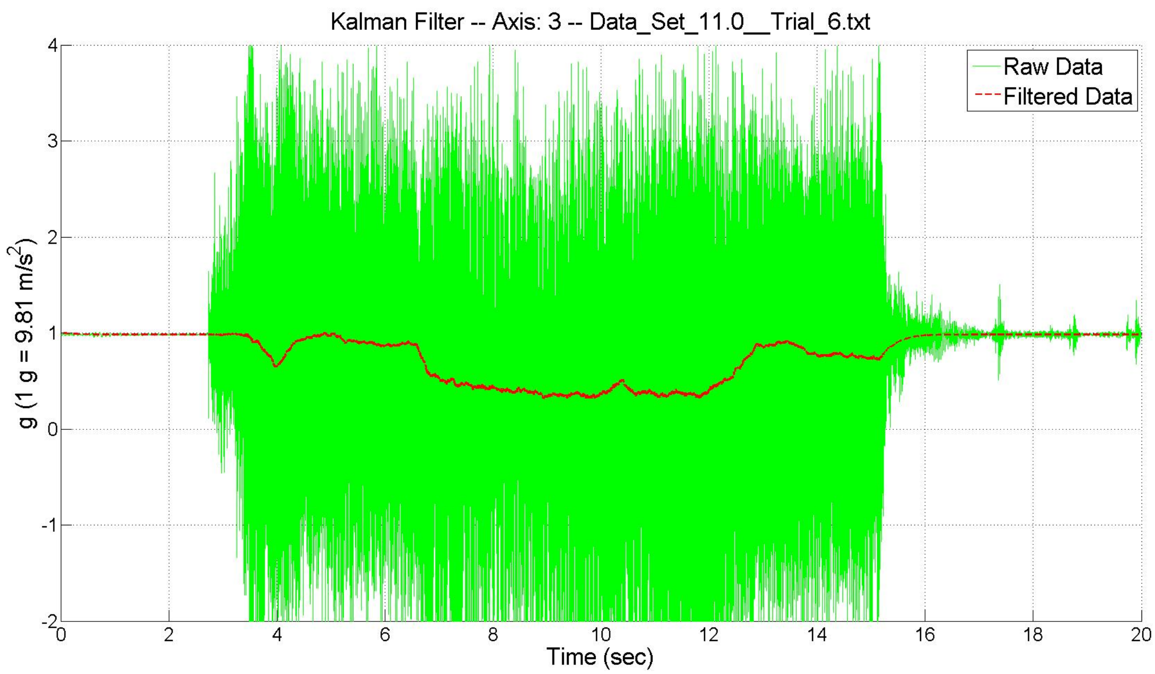

Figure 2.10. Performance of Kalman filter applied to accelerometer vibration data

false positives of kickback.

2.2 Analysis of Kickback Statistics

In order to be able to develop functional requirements for the kickback detection system, statistical information about kickback events has to be extracted. Each kickback event is a process that depends on many different factors, including operator, materials, tool condition, and even environmental influences. Therefore each kickback event has different characteristics. Although it is not possible to define a kickback event in a deterministic manner, it can be defined statistically, such that system requirements can be developed.

To accomplish this, data collected from the experimental trials has been analyzed to determine the following characteristics of kickback events overall:

- event duration,

- kickback velocity profile, and
- projectile impact energy.

Determining the kickback event duration is a critical part of this study. This duration essentially tells how much time passes from the point of kickback start to the point the work piece is ejected from the tool. The end of the kickback, the point of ejection, is also referred to as the time of separation. It is important to note that as defined, the start of the kickback is the point at which the feed velocity of the work piece reaches zero. This means that the actual kickback process, binding and energy exchange has already begun. In turn, this means that the calculated kick back duration is shorter than the entire kickback process. This is acceptable because a shorter duration only serves to tighten the functional requirements of the system, and can be thought of as introducing a small margin of error in the data collection and analysis process. Another advantage of defining the kickback start at the point of zero feed velocity is that it eliminates ambiguity and subsequently imprecise choices for the point of kickback start. This is because the start of binding is not an instantaneous event; it gradually increases over the course of several milliseconds. Attempting to select a consistent point between different trials would be unsuccessful. Figure 2.11 shows a histogram of the kickback durations for the analyzed data set.

The results show the average kickback duration to be about 90 milliseconds, which is in line with previous estimates, with a range of about 43 ms to 141 ms. This indicates that although variation is observed due to uncontrolled factors, there is satisfactory consistency in the process; where satisfactory refers to the limited variation in kickback durations, which in turn means that it should be possible to develop a system to react within the duration of the kickback.

An important observation to be made from this data is on the ability of a

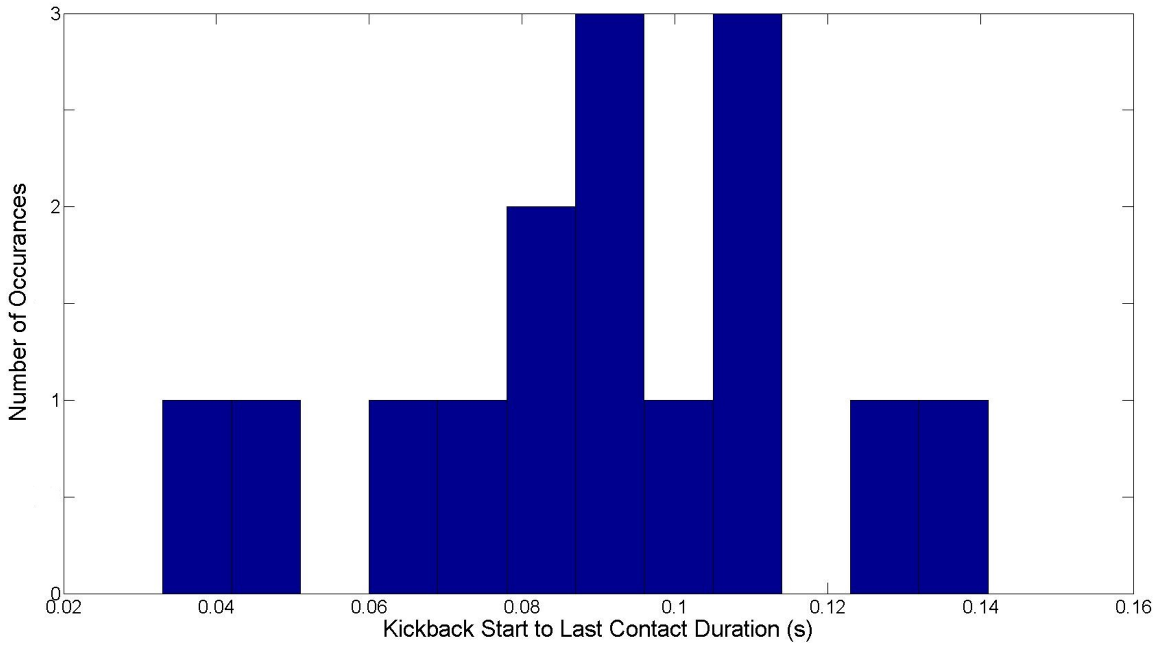

Figure 2.11. Histogram of kickback durations

tool operator to respond to a kickback event without any additional technology. Researches have confirmed the mean reaction time of college-age individuals to visual stimuli is 180 to 200 milliseconds [Wel80] and the reaction to touch stimuli is about 155 milliseconds [Rob34]. In the case of a kickback event, the operator is most likely to feel anomalies in the cutting process before anything is visually indicated, thus the reaction time for touch can be discussed. Comparing the reaction value of 155 milliseconds to the mean full kickback duration of 120 milliseconds indicates that an unprepared operator will not be able to perceive and react to an impending kickback in time. Essentially the kickback event will be fully completed by the time any reaction is attempted. This is simply due to the limitations of the human central nervous system, and is independent of the experience level of the operator. The only way the operator can alleviate or avoid kickbacks is by taking preventive steps such as properly setting up the tool and following proper cutting procedures.

The ultimate concern of an active safety system for detecting and potentially mitigating a kickback hazard is the damage that it may cause at impact. Since the kickback work piece becomes a projectile once ejected from the tool, it is important to know the velocity of the work piece at the point of ejection. This velocity is extracted from the velocity profile of the kickback as discussed in the following paragraphs.

As previously discussed, the velocity of the work piece is derived from its position data collected by the draw wire sensor. Figure 2.12 shows a plot of the velocity profiles of a few different experimental trials. The plot shows the variation in the velocity profiles that exists between different trials. The plots have been aligned such that the time of their zero feed forward velocities coincide.

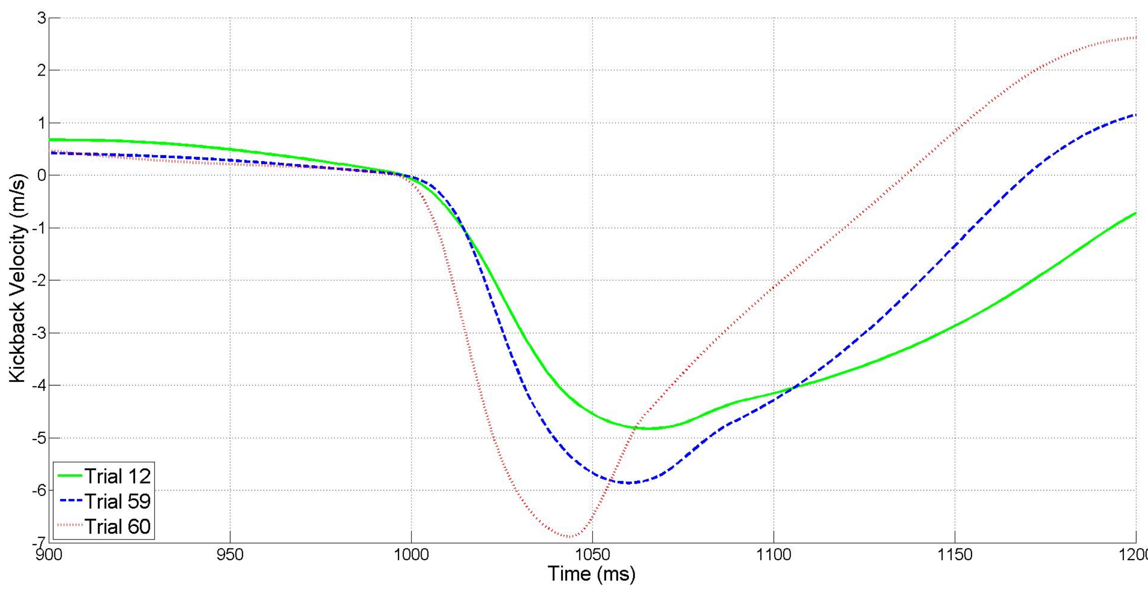

Figure 2.12. Velocity profiles of work pieces during kickback experiments

The plot shows two major areas of interest, the portion from the zero feed forward velocity to the point of separation is important because it shows what the work piece velocity is at certain time intervals after the kickback starts. This information is used to determine worst case scenarios for detection and mitigation, which is important because it is not necessary for the blade to stop instantaneously, it only needs to stop fast enough to prevent the work piece from reaching a kickback velocity over a predetermined allowable value governed by a threshold on the maximum projectile energy (i.e. impact damage potential). This in turn leads to the second area of interest, the time of separation. In a non-mitigated kickback, the time of separation corresponds to the highest velocity, projectile energy, and thus damage potential. In a mitigated kickback, the time of separation may correspond to the mitigated velocity, or there may be no separation velocity if the blade is stopped fast enough. To further aid in the statistical understanding of the exit velocities, Figure 2.13 shows a histogram of recorded values.

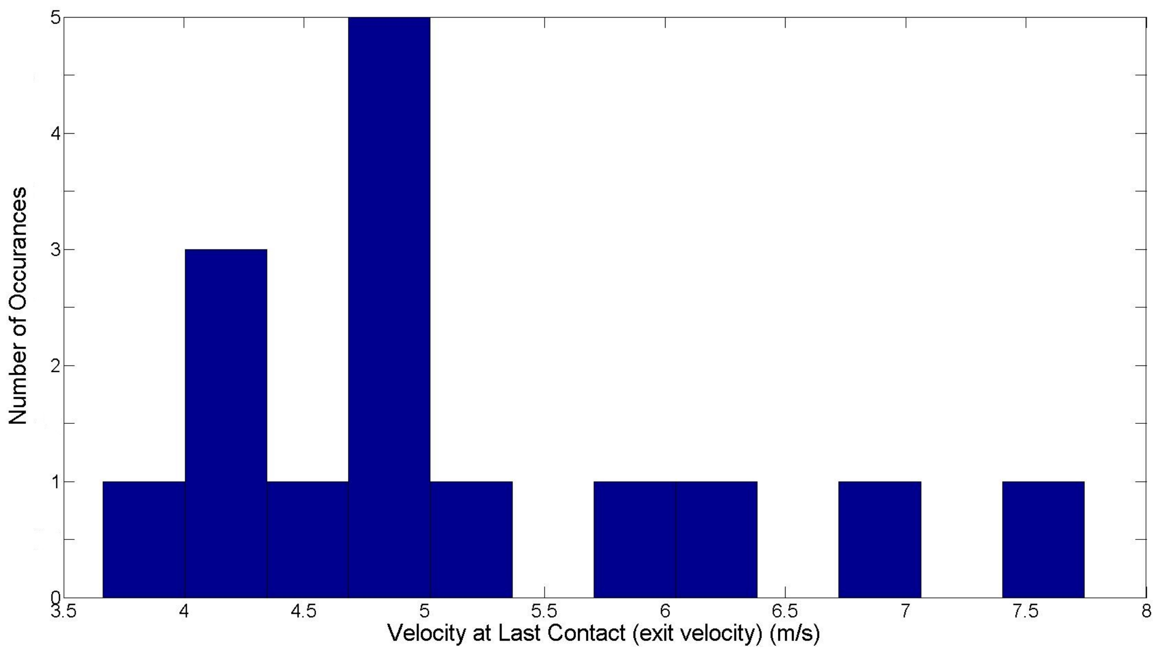

Figure 2.13. Histogram of kickback velocities at separation from saw blade

In order to use the velocity profile data to determine impact damage potential of projectile work pieces, a standard work piece needs to be defined. This is challenging and somewhat arbitrary, as there is no data to suggest what the most common size and mass of a work piece is. However, for this analysis, standard values are necessary. It can reasonably be assumed that one of the most common pieces of building material that professional contractors come across is the pine two inch by four inch stock. This is the most common structural material used in residential home construction to frame walls. Therefore, the following damage potential analysis will be performed with this material, having a mass of 1.90 kilograms per meter. It will be assumed that a rip cut is being performed (along the length of the piece) which is to be 1.22 meters long. This data is summarized in Table 2.5. It should be noted that contrary to the naming of the workpiece, a "2 inch x 4 inch" piece of lumber has the actual dimensions as listed in the table.

Table 2.5. Work piece properties for damage potential analysis

Property	Value
Material Type	Pine
Dimensions	1.5in x 3.5in x 48in
Weight	2.32 kg

Typically the projectile work piece has a translational velocity component as well as a rotational velocity component. The later is much lower in magnitude, and does not contribute significantly to impact damage, therefore this component will be assumed negligible or the analysis. Additionally, it is assumed that the potential energy of the work piece before and after the event is roughly equivalent and also negligible for the purpose of the following calculations. Further, losses due to air resistance will be assumed minimal due to a small time of flight (short distance to impact) and thus will be negligible. Therefore, the force of impact can be determined from the simplified work-energy relationship,

$$\mathbf{F}d = \frac{1}{2}m\dot{\mathbf{x}}^2 \tag{2.1}$$

where $\mathbf{F}$ is the impact force, d is the impact displacement (depth of travel), m is the work piece mass, and $\dot{\mathbf{x}}$ is the work piece separation velocity.

Using Equation 2.1 with the parameters of Table 2.5 the following plot is generated. Figure 2.14 shows the impact forces which are to be expected from a work piece with the predefined properties traveling at various velocities within the range of those observed during the experimental trials. Since the primary concern is bodily harm, rather than property damage, the equation will be calculated to reflect forced which may be generated when impacting the body. For this reason, the impact displacement (depth of travel) from Equation 2.1 is kept constant at 2 centimeters as referenced in a study on forces associated with lacerations and fractures [SCB+12]. Although this parameter, along with others which dictate the mechanism of skin or bone damage, will vary considerably depending where on the body the impact is, the chosen value is expected to provide a reasonable range for a majority of body areas.

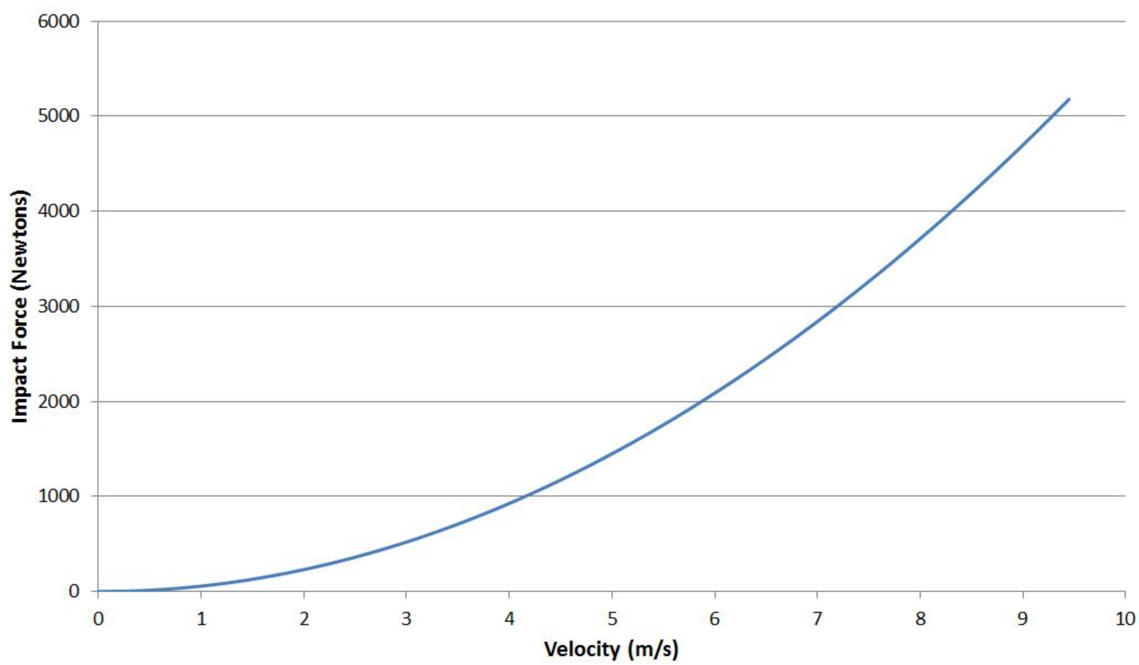

Figure 2.14. Impact force versus projectile velocity with standard properties

From studying Figure 2.14 and comparing to published forces causing laceration, which are in the range of 2,000–10,000 Newtons [SCB+12], it can be noted that projectiles having a velocity greater than 6.09 meters per second can cause lacerations.

2.2.1 Derived System Specifications. The analysis of the kickback data allows for the development of certain design requirements for the detection and mitigation parts of the safety system. As per the goal of the thesis, the two major concerns, or target goals, are the following:

1. Prevent injury due to ejected work piece (work piece kickback)
2. Prevent injury due to hand being pulled in towards the blade (work piece rotation)

Since this project is part of a research and development effort for a potential production product, certain restrictions need to be taken into account such that the final outcome adheres to product design requirements internal to Bosch, which ultimately have the goal of developing high quality products for the consumer; these are referred to Critical to Quality (CTQ) requirements. These CTQ requirements arise from a development process termed Voice of the Customer (VOC) where design and marketing factors are introduced into the development process. The VOCs, which are not particular to this project and therefore will not be discussed here, were used to develop the following set of CTQ requirements:

1. Saw blade stopping time
2. Added weight must be less than current safety components related to kickback (i.e. kickback paws, riving knife)
3. Must not affect tool cutting performance nor normal operation of tool

The CTQ requirements developed are now used to develop design requirements. Although weight is a very important requirement from the customer's point of view, especially in terms of portable tools, there is no need to develop a design requirement for this since the only components added are electronics and sensors. These components are far less massive than the current safety components used on the tool, less than 22% of the safety devices' mass (excluding rip fence). The CTQ requirement for the for the safety system to not negatively effect the normal operation of the tool means that the active safety system should avoid falsely triggering (i.e. false detection) to a high degree. This is very important in safety systems because excessive false triggering will lead to inconvenience to the user who will eventually attempt to disable the safety system, exactly the same response as would be produced toward a passive safety device which interferes with tool use. However this parameter does not have to be evaluated and can be set to a reasonable initial value of a maximum of 0.1% false detection, representing a false trigger every one out of 1,000 tool uses. Additionally, the CTQ requirement for the active safety system to not negatively effect the tool cutting performance does not need to be explicitly considered to develop separate design requirement because the system developed here will not be in a position that it can case changes in tool performance. Since the system will not have variable control of motor parameters such as speed, power, or torque but instead only a capability to stop the blade, this CTQ requirement essentially reverts to that of avoiding false triggering.

With the considerations discussed in the preceding paragraph, it is shown that the only CTQ requirement having significant influence on system design specifications, in terms of addressing the major concerns presented at the beginning of this subsection, is the saw blade stopping time. The stopping time is one of the most critical objectives of the project, because unless the kickback is mitigated (blade stopped) within the required time, there is nothing else that can be done to prevent the kickback of a work piece at a dangerous velocity. Also, during many kickback incidents, the workpiece can translate and rotate in a number of different ways. During every single kickback, the work piece translates, is ejected, in the direction towards the user (i.e front of the tool), this is due to the direction of blade rotation and is influenced by few other factors. However in some cases, depending on the work piece geometry and orientation relative to the saw blade — mainly the relative location of the work piece center of mass and force applied by the saw blade — the work piece can experience a rotation. During such an occurrence, if the tool operator has one hand behind the blade in order to pull the work piece out of the tool, as is commonly though in appropriately practiced, then there is a chance that the work piece, as it rotates and simultaneously translates, can pull the operator's hand directly into the saw blade [CP11]. This is the reason for the second major concern as presented in the beginning of this subsection. The stopping time requirements for the two target goals may be different, and the shorter allowed time will be taken as the design requirement.

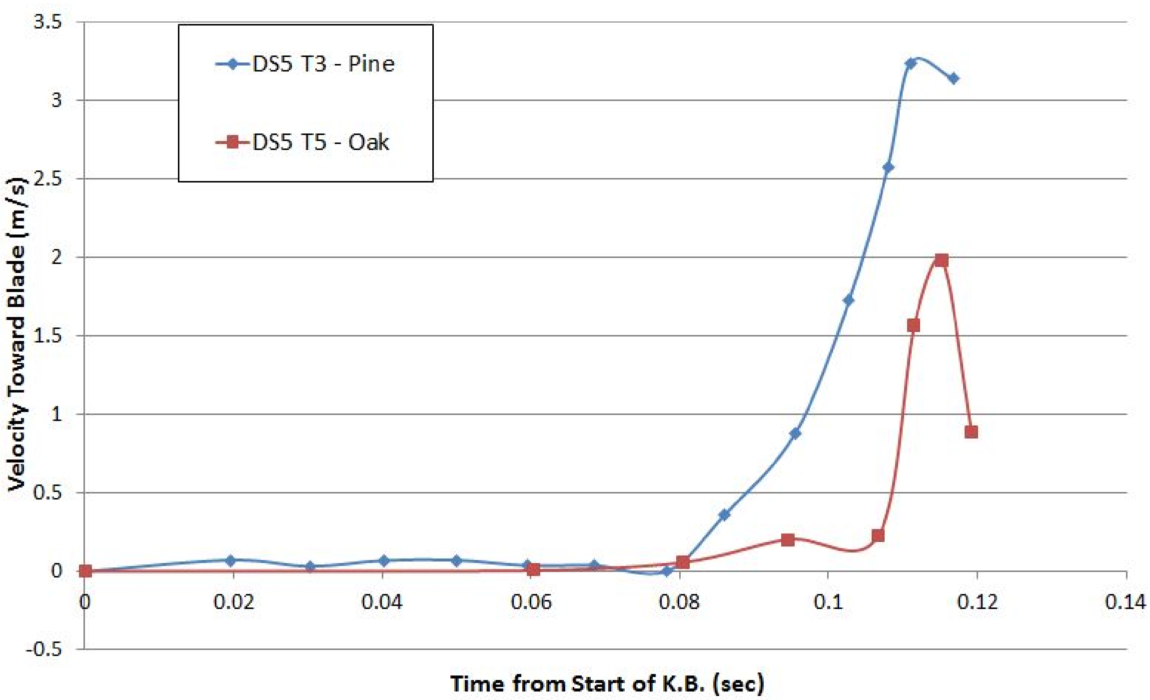

Figure 2.15. Work piece lateral velocity profile during kickback experiments

Determining the time requirement to address the concern of work piece rotation is determined by analyzing plots of the lateral — translation perpendicular to blade due to work piece rotation — workpiece velocity as shown in Figure 2.15. An important note about the lateral velocity is that it very much depends on where it is measured (where the operator's hand is). It has been observed that much of the lateral velocity occurs once the work piece lifts up and is pulled over the blade, which is towards the end stage of the kickback. Although the two trials presented in the plot have a very similar profile of the lateral velocities, there can be a significant amount of variation, which is taken into account by introducing a safety margin. It can be seen in Figure 2.15 that the lateral velocity does not have any significant magnitude until 0.080 seconds, therefore a conservative value with 30% safety margin is chosen, which is 0.0525 seconds and is set at the maximum stopping time threshold for this criterion (due to rotation).

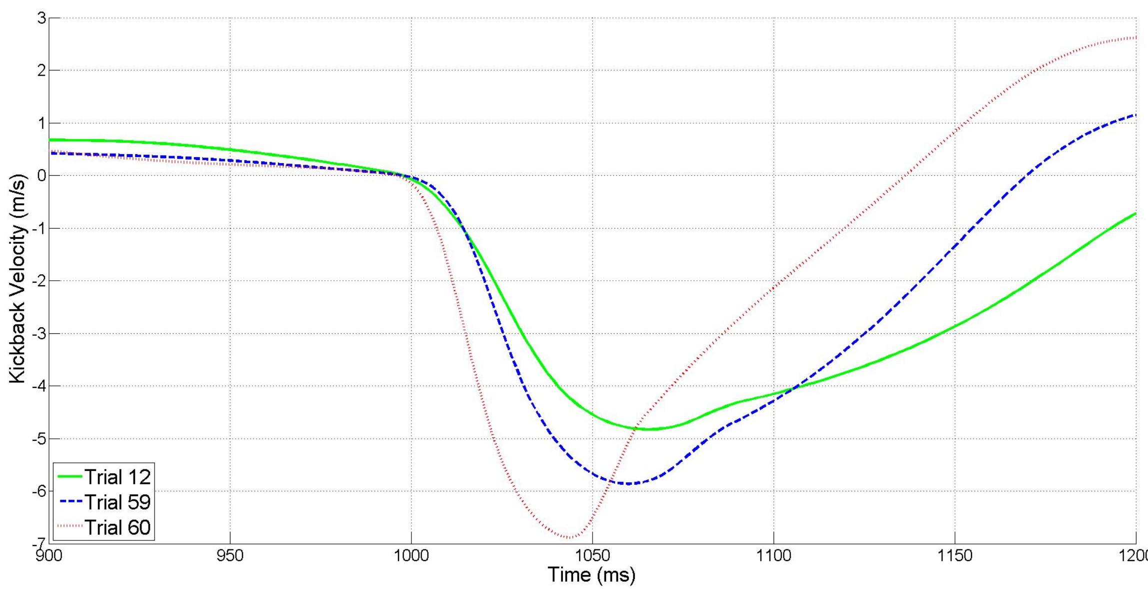

Figure 2.16. Velocity profiles of work pieces during kickback experiments

The time requirement for stopping the blade due to the concern of work piece translation, alternatively concern due to impact damage from kickback projectile, is determined using the $6.09\frac{m}{s}$ threshold found in Section 2.2. As shown in Figure 2.16 this corresponds to 30 milliseconds after kickback start (by definition); however, not all kickbacks have a velocity higher than this value as shown in the histogram of Figure 2.13. Regardless, this threshold is used to determine that based on this mode of kickback, the time requirement to stop the blade is 30 milliseconds in order to keep bodily damage below the potential for laceration, which still means that injuries such as bruising can occur as well as significant pain and injury to delicate parts such as contact with facial areas. A safety margin is not applied here since only a small percentage of kickbacks reach this velocity.

By combining the two stopping requirements and choosing the smaller values, given by the restriction on impact damage, the blade stopping requirement for an effective detection and mitigation system is 30 milliseconds.

2.3 Applied Detection Methods

The following section discusses the implementation of the kickback detection methods, which are later evaluated for performance in Section 3.1.

2.3.1 Angular Acceleration Based Detection. One of the simplest methods for detection explored for this application is referred to as a simple threshold detection. The goal with taking this approach is to investigate the effectiveness of a system in which the detection method is simple and thus the electronics can be simple and cost effective. This naturally translates into a system with a fast and computationally robust response by the decision making portion of the software.

The method involves acquiring data, processing it, and then comparing it to pre-established thresholds which would indicate a kickback. The challenge with this method is establishing which signals vary such that it correlates with a kickback event. An additional challenge is determining what the threshold should be set to, such that it is not falsely triggered during normal cutting operations. The available signals to evaluate are the blade angular velocity, the three axis acceleration from the accelerometer (X-acceleration, Y-acceleration, and Z-acceleration), and any derivatives of these signals, such as the angular acceleration of the blade.

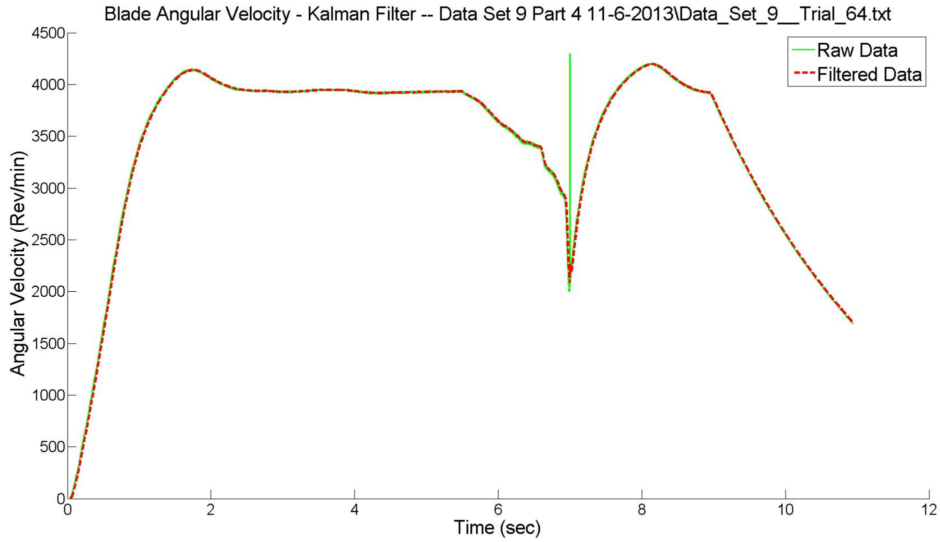

(a) Full range

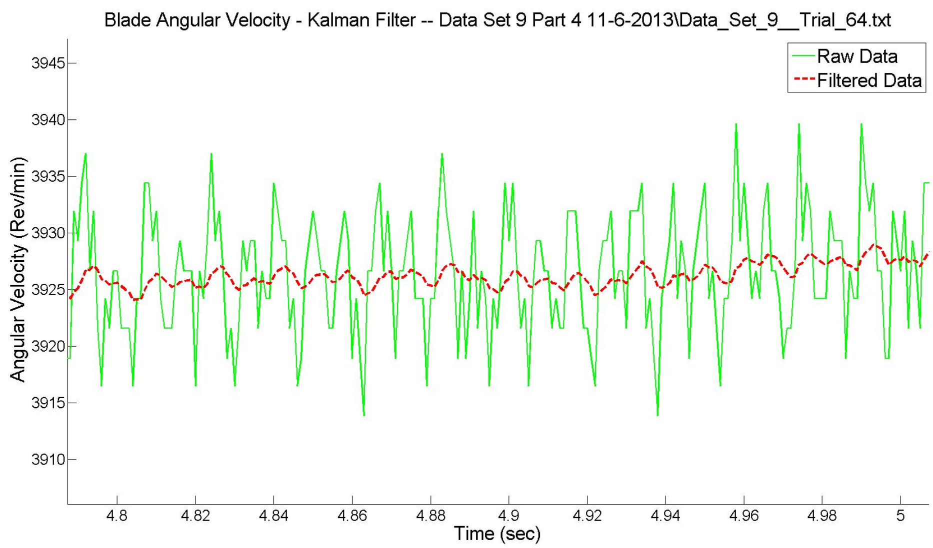

(b) Zoomed in to $t = 4.8s\ to\ 5.0s$

Figure 2.17. Result of applying Kalman filtering on angular velocity data

Before the data is analyzed it is processed through a Kalman filter as discussed in Subsection 2.1.2. The result of filtering the data is shown in Figure 2.17, in which the solid line indicates raw data, and dashed line is the filtered result.

Although the need for filtering of the angular velocity may not be immediate in itself, when taking into account that this data is then derived to produce the angular acceleration it becomes evident that without filtering the detection based on an acceleration threshold is not possible. This is due to the high frequency noise in the raw data, which is substantially magnified when derived. Figure 2.18 shows this result and the effect of filtering, in which the filtered signal is overlayed onto the raw signal.

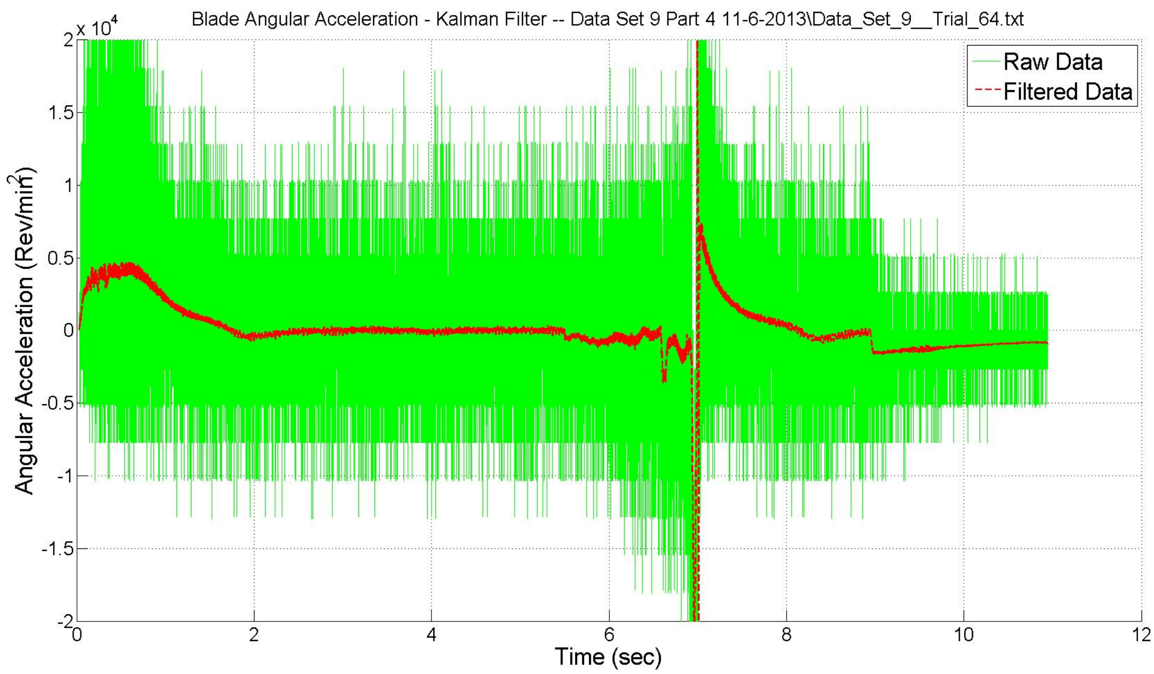

Figure 2.18. Angular acceleration derived from angular velocity

Various combinations of input data were considered with this method. The performance is best when comparing the angular acceleration, $\boldsymbol{\alpha}$, of the blade against a threshold. Including any other data does not significantly improve the results. This was expected, as the kickback event causes a considerable and quick drop in the angular velocity of the saw blade. The angular velocity however, did not establish a clear region of normal operation versus a kickback event and was not useful to include in this method; this meaning that the operating range of the tool speed varies substantially during normal use, as does the speed range over which kickbacks occur. Through evaluation and comparison of data between kickbacks and normal cutting (baseline cuts), it has been found that a good choice for the angular acceleration threshold would be $\Gamma = -3,750\frac{RPM}{sec}$. This same value is used in the performance evaluation of the method in Subsection 3.1.1.

2.3.2 Vibration Based Detection. A different method of kickback detection deals entirely with the frequencies generated by the tool and their variation over time. The purpose of developing this method is to investigate the ability to successfully perform kickback detection using only an accelerometer (for vibration data). This can be a preferred alternative in many implementations due to the ease of implementation and cost. The physical implementation of vibration monitoring using an accelerometer is simply done by embedding an accelerometer at appropriate locations within the tool. Appropriate locations offer a rigid connection to the tool's motor/gearbox assembly while simultaneously avoiding locations that resonate excessively. Appropriate locations differ from one tool to another because of variations in construction, however for the test tool used in this project, the Bosch GTS 10 XC, an appropriate location offering a good signal to noise ratio was the gearbox. On this particular tool, the gearbox is aluminum, which not only contains the gearing to provide the speed reduction but also serves as an intermediate body between the motor and the undercarriage assembly, as shown in Figure 2.19.

This location provides excellent access to vibrations of interest; however, it also allows for the noise from the motor commutation and resonating bodies to be picked up as well. For the purpose of this project, the frequencies of interest in the tool have been identified in the region of 50 Hz to 500 Hz, corresponding to rotating components such as the saw blade, shafts, gears, and motor armature. The corresponding frequencies of the major components are noted in Table 2.6.

The noise at this particular mounting location has been found to be at frequencies much higher than those of interest, thus they are not a considerable problem.

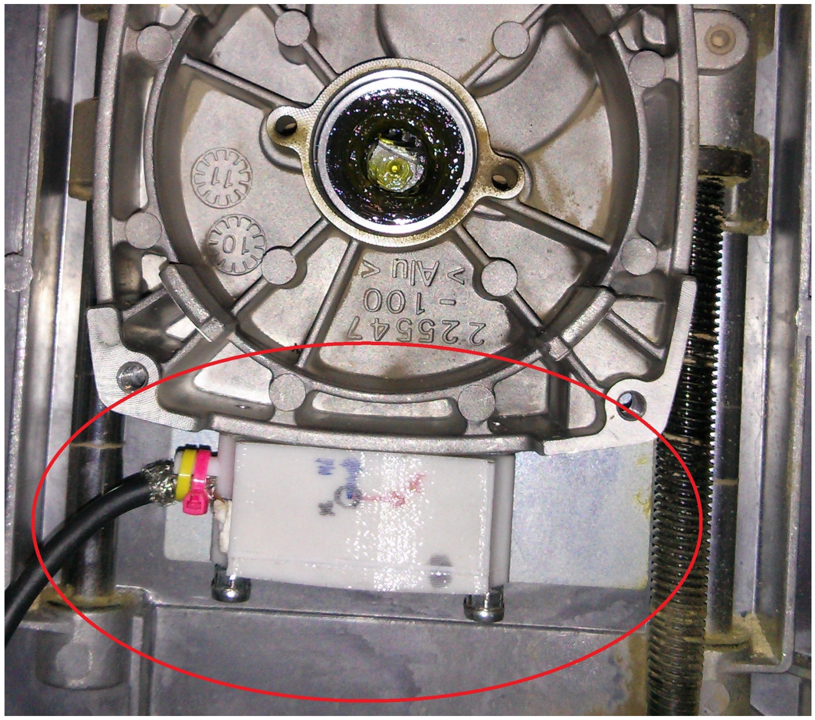

Figure 2.19. Accelerometer attachment to underside of gearbox

As mentioned previously in Section 2.1, the application of a micro-electromechanical system (MEMS) accelerometer is not ideal in this case. This is due to the effects large alternating vibrations have on the DC Bias of the MEMS accelerometer. This offset can be noted in Figure 2.20, showing large low frequency (DC) offsets of the mean of the signal. However, it has been found that since we are not interested in these low frequency components, applying a high-pass filter with a frequency stop above 10 Hz can eliminate this offset. Further, it should be noted that for the purpose of frequency based detection, applying the high-pass filter to remove the DC bias errors is not necessary because the other frequencies of interest are not affected.

At this point, no further signal conditioning is required to process the vibration signal. The remaining procedure deals with evaluating the magnitudes of the different frequencies from the three orthogonal axes, and comparing them to the predetermined patterns of a likely kickback.

Table 2.6. Frequencies corresponding to rotating components

Component	Frequency (Hz)
Saw Blade	62.5
Arbor Shaft and Output Gear	62.5
Input Gear	375.0
Armature	375.0

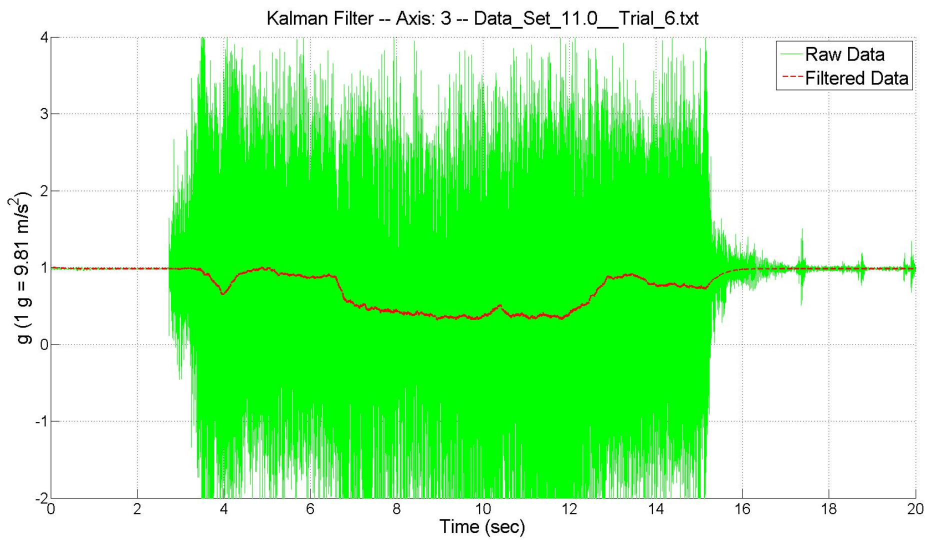

Figure 2.20. Results of filtering accelerometer data and effect of DC offset drift

The technique used for obtaining the magnitudes of the various frequency components is the Fast Fourier Transform (FFT) method. Utilizing this method, as described by the Cortex Micro-controller Software Interface Standard (CMSIS) Digital Signal Processing (DSP) Library [ARM] provides the frequencies in groups, or bins, and the magnitude of the bin. In order to optimize the detection time versus the resulting frequency resolution, the FFT is provided with the latest 128 samples. This implementation provides the decision making portion of the software with the frequency magnitudes bundled in a number of bins which make it efficient to compare against thresholds.

Based on comparisons of frequency response from baseline measurements, the

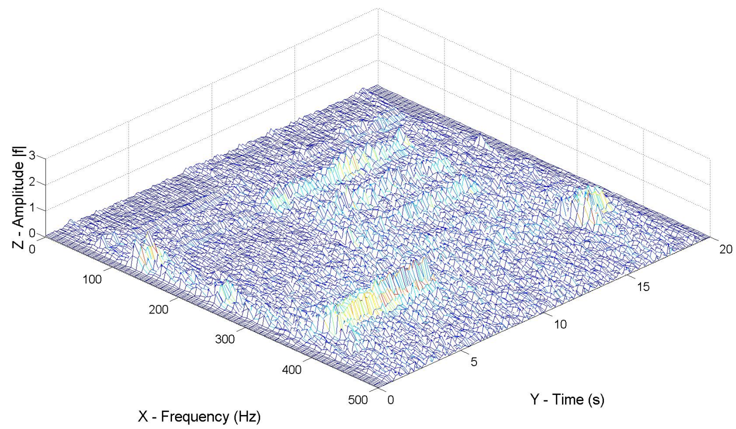

(a) X-Axis

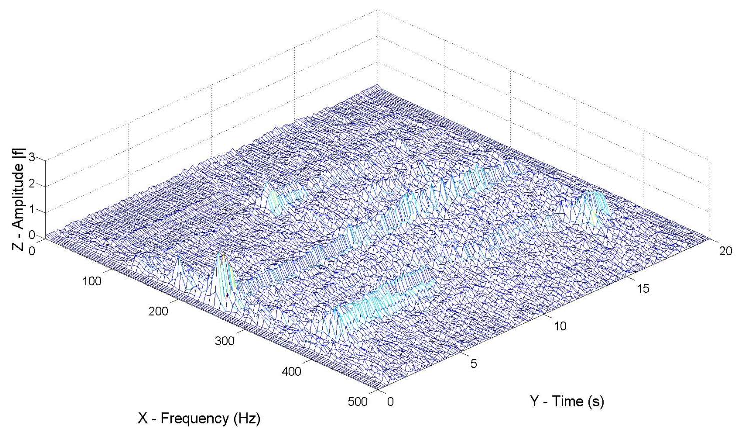

(b) Y-Axis

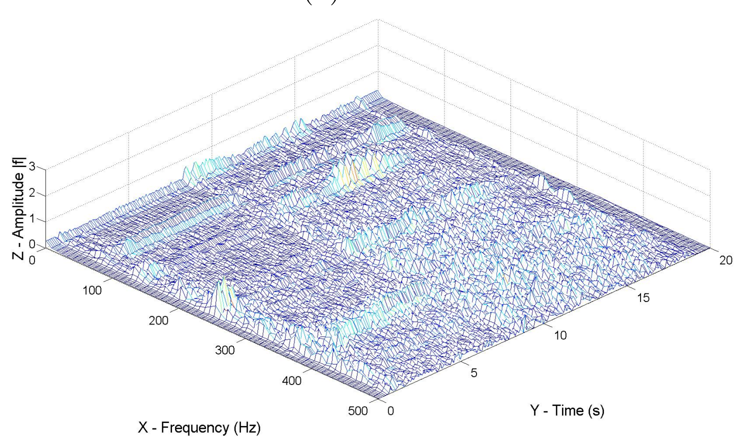

(c) Z-Axis

Figure 2.21. FFT results from accelerometer during baseline data collection

detection thresholds can be computed. The baseline measurement involve collecting frequency data with the tool in use under different circumstances, but not generating

Table 2.7. Frequency threshold settings

Frequency Component	X-axis Mag.	Y-axis Mag.	Z-axis Mag.
60 Hz	< 0.2	N/A	< 0.2
242 Hz	< 0.4	> 0.5	N/A
375 Hz	N/A	< 0.2	N/A

any kickbacks, as is shown in Figure 2.21. Various methods exist for determining the settings of the thresholds, and for this project the approach was to visually inspect the FFT plots and determine effective combinations of frequency threshold. Table 2.7 lists the frequencies found to be indicative of a kickback event.

It will be necessary to further refine these threshold for conducting performance testing or if any components are altered. This is one of the drawbacks of using a frequency based method when any modification of the tool's physical characteristics can potentially have substantial effects of the vibration signature.

CHAPTER 3
EXPERIMENTAL VERIFICATION

In this chapter, the detection methods presented in Section 2.3 are evaluated for performance.

3.1 Detection Performance

In this section, results from experimental performance testing are presented and discussed. Two methods are evaluated: blade angular acceleration and vibration monitoring. The performance testing is conducted on the same setup as discussed in Chapter 2 and the detection algorithms described in Section 2.3.

3.1.1 Angular Acceleration Performance. The performance of the detection method based on the saw blade angular acceleration is presented and discussed in this subsection. The main evaluation parameter for all of the detection methods is the time delay in detection. As discussed earlier, this time delay represents the duration until detection relative to the kickback start time, which has been defined as the initial moment that the work piece develops a negative feed velocity, or alternatively the zero velocity point. This is important to note, because as is discussed in the following test and figures, there are instances where the detection time is negative, which means that the threshold has been exceeded before the work piece had a zero or negative feed velocity.

The sole variable parameter of this detection method is the value chosen as the angular acceleration threshold, Γ. Any acceleration beyond this is registered as a kickback, which in a fully function mitigation system would trigger physical mechanisms to stop the saw blade. For the purposes of this performance testing, the setting will be $\Gamma = -3,750 \frac{RPM}{sec}$. This value has been developed based on the procedure discussed in Subsection 2.3.1. Additionally, the performance testing is conducted with the same procedure as for generating kickback during data collection.

Figures 3.1 and 3.2 show the angular velocity (RPM) of the saw blade for two separate trials, with the plot zoomed in to the kickback region. The vertical lines in the plots indicate the following events:

- Kickback detected (dashed line)
- Start of kickback per definition (solid line)
- Work piece separation from saw blade, i.e. last contact (dotted line)

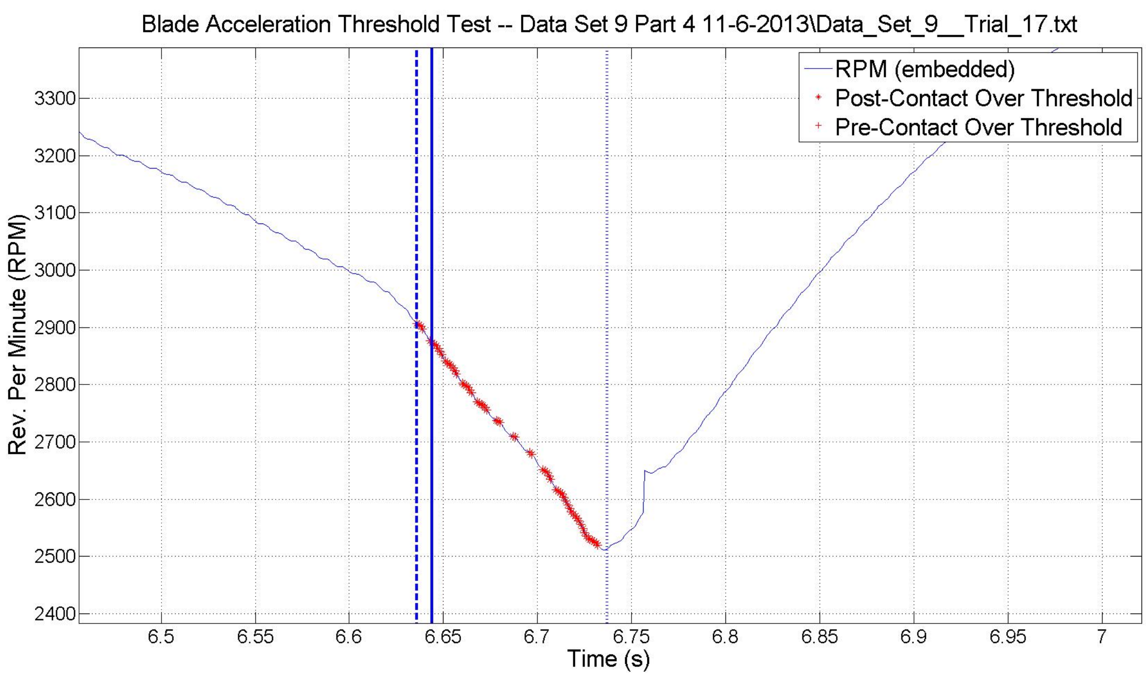

Figure 3.1. Example of detection prior to kickback start

Figure 3.1 is an example of a case where the kickback is detected some time before the start of the kickback, meaning that the detection occurred before the work piece lost all of its forward feed velocity. However it can be seen in the plot that the

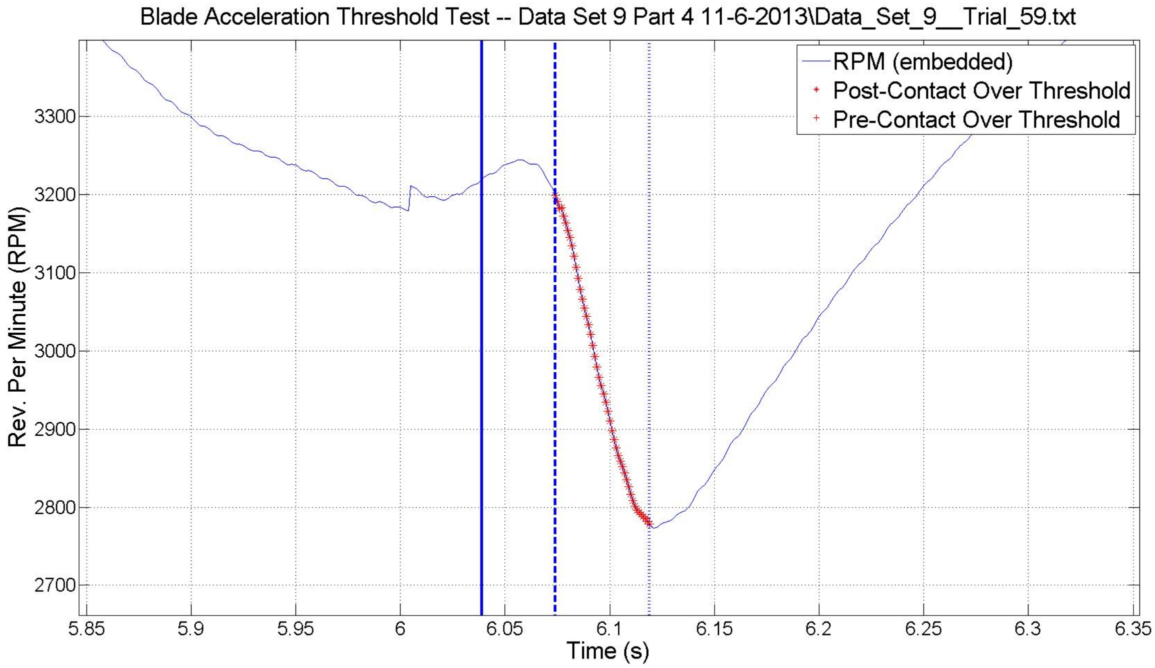

Figure 3.2. Example of detection after kickback start

actual kickback process has begun long before this as is indicated by the continuously decreasing slope of the angular velocity (RPM) curve.

Figure 3.2 is an example of a case where the kickback is detected after the start of the kickback, thus the workpiece has already began to move backwards. This particular trial is interesting in that the angular velocity (RPM) pattern differs from the typical continuously decreasing slope, instead having a range where it increases. This is due to experimental setup parameters that are not under control, parameters which ultimately effect the dynamic interaction between the saw blade and the work piece. Such parameters include exact work piece trajectory leading to the very influential interaction between the blade teeth/body and the edges of the kerf in the work piece, the varying material properties throughout the length of the cut, and any other physical factors which vary the amount of traction developed between the two bodies.

An overall sense of the performance of this detection method can be observed by the distribution of detection times. Figure 3.3 shows this distribution, which is a measure of the elapsed time between detection and the start of the kickback as has been defined.

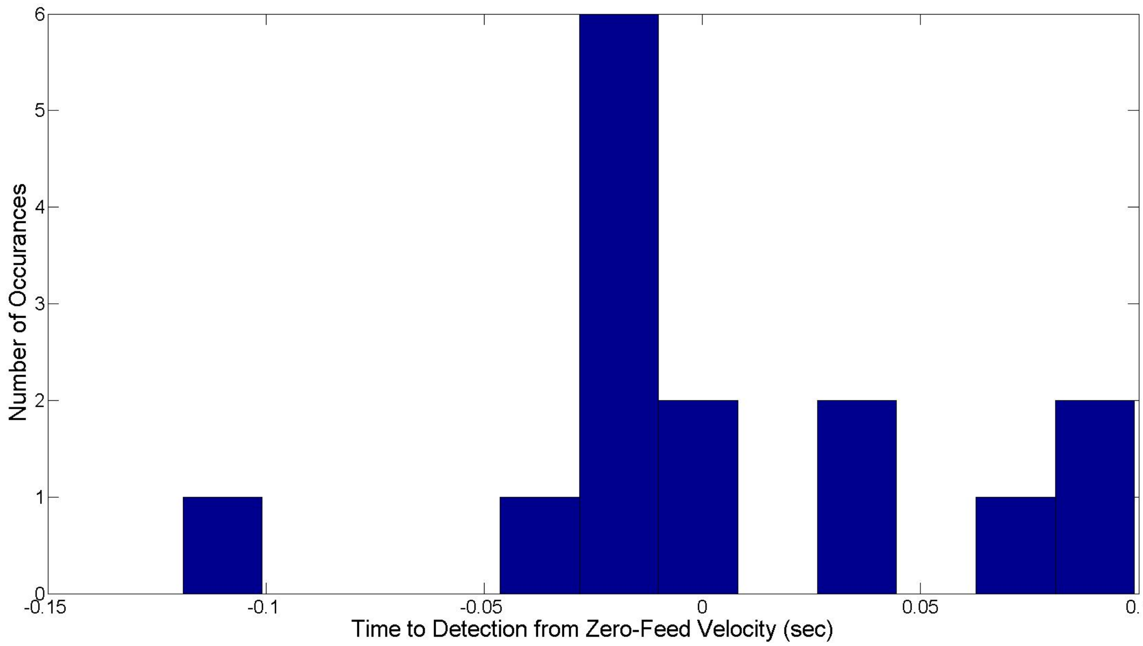

Figure 3.3. Histogram of time to detection (angular acceleration method)

A notable result is the large number of occurrences of detection prior to the start of the kickback. This is very good indication towards the performance of this methods. This histogram represents data from fifteen different trials performed as part of the performance evaluation data set. Statistical properties of these results are further summarized in Table 3.1.

Though this method has a very good overall detection rate, it does suffer from large deviation which is a potential issue in terms of safety system design. In such an application, the method must be developed to a point where it can be expected to perform in a very tight error tolerance. To achieve this, further development needs to be performed, especially further study with control of more parameters. Controlling more parameters during experimentation and design will have no effect

Table 3.1. Detection statistics of angular acceleration threshold based method

Detection Stat.	Value
Mean	3.1 ms
Median	-13.0 ms
Maximum	99.0 ms
Minimum	-119.0 ms
Standard Deviation	55.4 ms
Variance	3.1 ms

on how the tool is used in practice; however, something may become evident from a more inclusive study which may potentially improve performance. Another potential way to improve detection would be to further reduce variations in the angular velocity signal such that the angular acceleration curve is smoother and allows for the more precise tanning of the detection threshold. Alternatively, combining this method with that discussed in Subsection 2.3.2 and evaluated in the following section, may provide further stabilization of the detection performance.

3.1.2 Vibration Detection Performance. The performance of the detection method based on vibration frequency thresholds, which is detailed in Subsection 2.3.2, is presented and discussed in this section. As discussed previously, the main evaluation parameter for all of the detection methods is the time delay in detection. This time delay represent the duration until detection relative to the kickback start time, which has been defined as the initial moment that the work piece develops a negative feed velocity, or alternatively the zero velocity point.

The threshold parameters used for performance evaluation with this method are listed in Table 3.2. These have been developed as discussed in Subsection 2.3.2. The biggest challenge with this method has been found to be environmental noise, which includes resonance noise from the tool itself as well as external environmental interference, however it has been additionally noted that the frequency response recorded is sensitive to environmental conditions such as temperature and humidity. For these reasons, and due to setup relocation, the noted thresholds for this performance evaluation varies from those previously discussed.

Table 3.2. Frequency threshold settings for performance evaluation

Frequency Component	X-axis Mag.	Y-axis Mag.	Z-axis Mag.
60 Hz	N/A	N/A	< 0.2
117 Hz	> 0.5	> 0.8	> 0.6
242 Hz	< 0.4	> 0.5	N/A
375 Hz	N/A	< 0.2	N/A

With the settings and setup as discussed several performance trials were conducted. An example of the frequency results of a single trial, where the shaded plane marks the detection time at 6.093 seconds, is shown in Figure 3.4. The three vibration axis are individually computed and processed against the thresholds. An important note regarding Figure 3.4 is that this figure has been generated after the performance trial using the data which was recorded and with the actual time of detection shown. This is necessary for illustration because the frequency components evaluated with the embedded FFT software is are not stored due to the excessive amount of data that is generated.

For this particular trial, the delay in detection relative to the start of kickback as defined by the zero feed velocity of the work piece is 24.04 milliseconds. The interesting advantage of this method is the relative consistency in detection time that it provides. Although it has shown to have a longer delay in detection, the variation in detection time is low relative to the other method, which in safety systems is important. An important note about the statistics presented for here is the limited number of tests performed, a total of six trials. This amount is not statistically

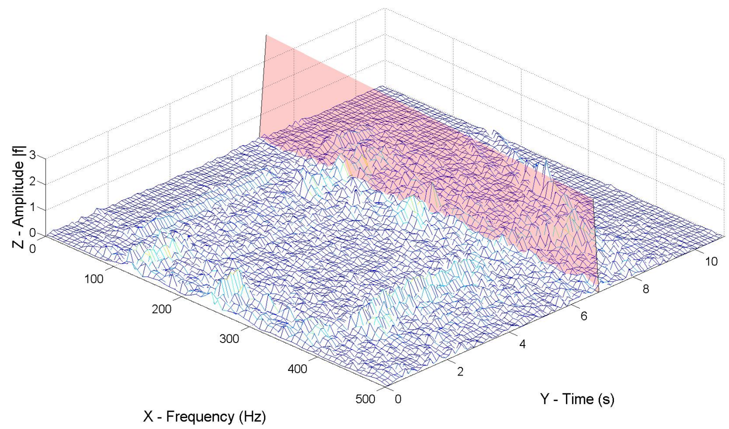

(a) X-Axis

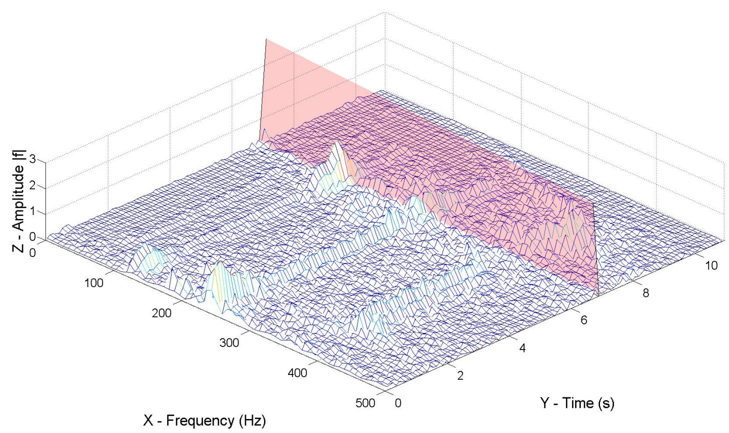

(b) Y-Axis

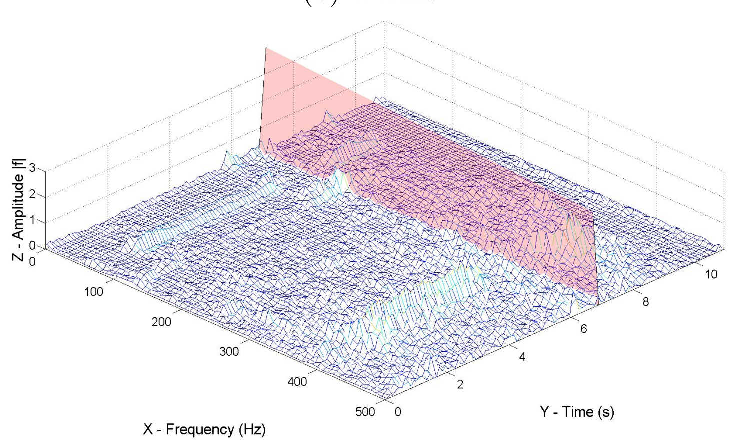

(c) Z-Axis

Figure 3.4. FFT results from accelerometer data during a kickback

significant; however, it is still a good indication as to the performance potential of the method. The result of the statistical evaluation is presented in Table 3.3. This data is also illustrated as a histogram in Figure 3.5.

Table 3.3. Detection statistics of frequency threshold based method

Detection Stat.	Value
Mean	50.11 ms
Median	33.26 ms
Maximum	63.46 ms
Minimum	17.68 ms
Standard Deviation	15.97 ms
Variance	0.25 ms

The results from this performance evaluation on the detection method based on tool vibration frequencies are interesting in that the results are more consistent between trials as opposed to those of the angular acceleration method. The low number of trails is an issue in solidifying the performance evaluation of the method, however it serves as a good indicator. The long delay in detection is to be expected, since there is lots of variation in the magnitude of the frequency response as computed by the FFT, the thresholds were necessarily set loosely to prevent false detection. The potential for precisely tuning this method to the application is quite evident, and very possible by employing some further signal processing strategies. Isolation of noise is essential, thus further evaluation of accelerometer mounting positions may be beneficial.

As discussed in the preceding section, a combination of the two methods may provide a combination of the advantages that the methods individually provide. Fast detection system, having the robust precision of this method, would be an excellent performer. In the safety systems field, it is evident that delayed, or no detection, is just as bad as false detection. Due to the nature of people, a system that falsely

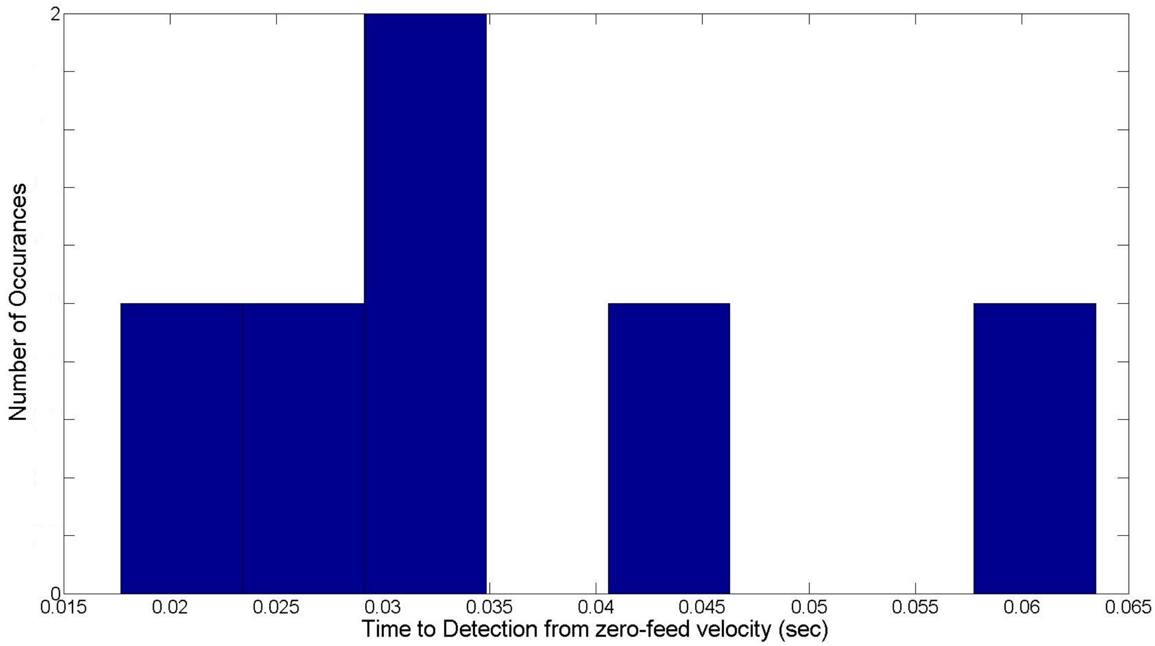

Figure 3.5. Histogram of time to detection (vibration monitoring method)

triggers consistently will not be tolerated, even if it also prevents actual injuries.

3.2 Integrated Detection and Mitigation

In the interest of producing a well rounded and evaluated system, a performance test with a physical mitigation method is described here. This integrated evaluation will be performed with the detection method based on the saw blade angular acceleration threshold, in conjunction with an experimental brake designed for emergency braking of power tools.

This brake design is interesting in that it is based on principles of centripetal forces, thus will be referred to as the CR brake, and takes advantage of certain geometries to enhance its braking effect. The CR has been developed externally to this project and is described in detail in a number of literature and patent publications [Win11a, Win09, Win11b]. The published performance characteristics of this brake are quite impressive, with time to complete stop ranging in the tens of milliseconds. However, the prototype provided for this test has been used beyond its designed

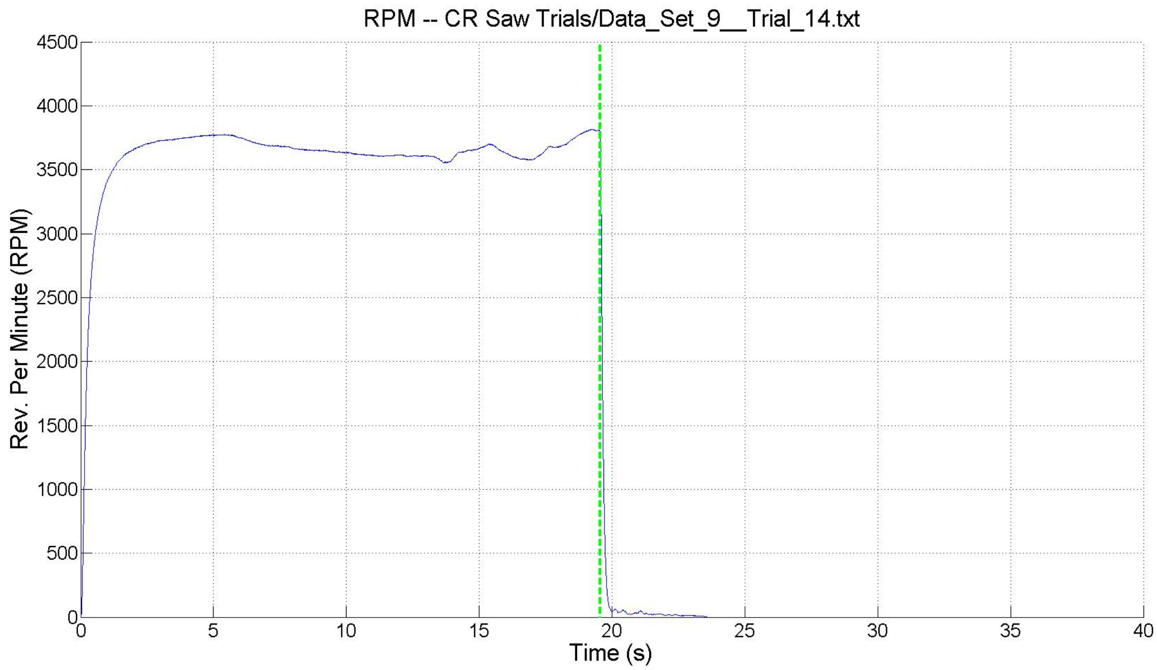

Figure 3.6. Mitigation with angular acceleration detection and the CR brake

nominal life, thus such braking times are not expected. The goal here is merely to obtain a starting point for understanding the performance of an integrated system.

Figures 3.6 and 3.7 show the results from one of the integrated system performance tests. Although the CR brake did stop the blade faster than could be perceived, the data for this particular showed that the braking duration was actually about 310 ms long. Additional trials following this resulted in even longer braking times due to the excessively work components.

The time of detection, which can be noted in Figures 3.6 and 3.7 as the dashed vertical line, had a delay of about 16 ms which is well within expectations.

Overall the integrated system performed well, however the braking effort was not strong enough to prevent the work piece from kicking back. Further integrated performance testing needs to be performed, not only to verify detection and braking times, but also to determine details such as communication delays and triggering

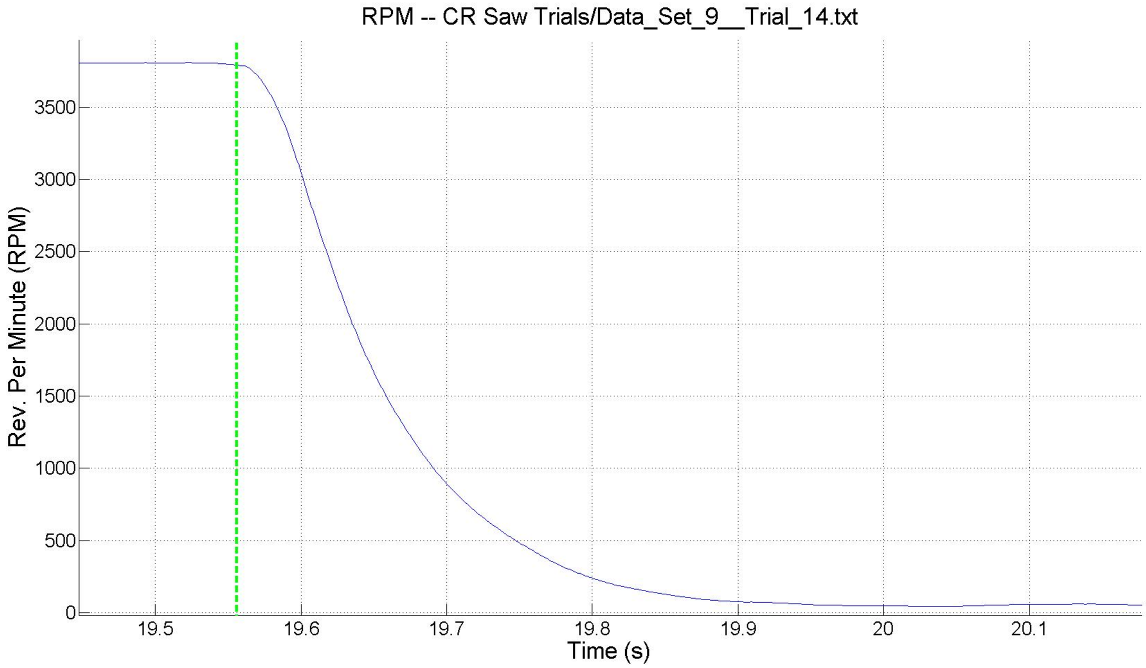

Figure 3.7. Zoomed in on braking event of Figure 3.6

methods. It has been noted during these trials that delays in triggering and communication can amount to a few milliseconds, which can be quite significant.

CHAPTER 4
CONCLUSION

The purpose of this thesis has been to conduct research and development of practical methods to detect hazardous kickback events and verify, in combination with mitigation methods, their effectiveness in completely or substantially reducing the damage potential. The ultimate result of a kickback is a projectile having a significant mass and velocity, and thus the potential to cause significant bodily or property damage. The main concern in evaluating damage potential has been in terms of bodily harm and has been evaluated based on the kickback projectile velocity. Since in general, the longer the work piece remains in contact with the power saw's spinning blade the higher the projectile velocity will be, the practical goal of reducing the damage potential is to detect the hazardous situation as early as possible and take steps to stop the spinning saw blade.

The detection time is thus a critical component of any active response technology in such an application. The reason for this being that the faster everything can happen, detection and mitigation, the less the damage potential will be, and similarly the faster detection occurs the more time remains for mitigation. This is the case because there is a relatively short window of opportunity where the spinning blade needs to be stopped. After this time, stopping the blade will do nothing to stop the projectile from continuing to kickback, as it has already acquired a significant amount of momentum. As part of this thesis work, this widow has been determined, although it may vary by a significant amount based on environmental variables, to be in the range of 20 to 30 milliseconds. This is a very short amount of time to detect an initially subtle situation and bring all spinning components to a complete stop. It is thus evident that every millisecond counts and increases the odds of mitigation significantly.

Developments in detection based on the saw blades angular acceleration and based on monitoring the tools vibrations have been presented and evaluated. Through experimental trials, both methods have proven effective in detecting an impending kickback within 12 milliseconds. This detection, although very fast, leaves a small margin of time to the mitigation step, in turn requiring high amounts of actuation effort. This performance however is acceptable under the goals of the thesis, as some mitigation methods that can stop the saws blade in under 10 milliseconds exist, and others are actively being developed.

As further development under this thesis, two concepts which could not be prototyped and experimentally verified, offer high potential in substantially reducing the detection time. One concept deals with applying machine learning to predict the state of the tool in the future, and the other involves a novel sensing method that has the potential to indicate an impending kickback before there are any physical effects that can be detected by the other sensors.

Suggested additional work on the project is to continue experimental verification of the presented detection methods on various tools under varying environmental and use variables in order to fine tune the methods. Additionally and strongly suggested, is to implement and conduct practical trials to verify the performance of the concepts presented under this thesis. The potential for substantially reducing the detection time is very high versus the cost of implementation.

APPENDIX A

KALMAN FILTER EQUATIONS

The following set of equations describe the Kalman filter implementation in this project. This is a discrete implementation with sampling period $T_S = 0.001s$. There are no control inputs but unknown disturbance inputs (noise) are taken into account.

The Kalman filter consists of two phases, measurement update and time update, which are evaluated continuously one after the other. During the measurement update, data (measurement $\boldsymbol{z}$) is acquired from sensors, which is used to calculate the new state estimate, $\hat{\boldsymbol{\zeta}}$ (see Equation A.3). Additionally, the update of the covariance is given by Equation A.1, in which $\bar{\boldsymbol{P}}$ is the covariance from the preceding time update, $\boldsymbol{H}$ is the state observation matrix, and $\boldsymbol{V}$ is the measurement noise covariance.

$$\hat{\boldsymbol{P}} = \bar{\boldsymbol{P}} - \bar{\boldsymbol{P}}\boldsymbol{H}^{\boldsymbol{T}}(\boldsymbol{V} + \boldsymbol{H}\bar{\boldsymbol{P}}\boldsymbol{H}^{\boldsymbol{T}})^{-\boldsymbol{1}}\boldsymbol{H}\bar{\boldsymbol{P}} \tag{A.1}$$

The Kalman gain, $\boldsymbol{L_K}$, is computed as shown by Equation A.2, where $\hat{\boldsymbol{P}}$ is the state covariance after the measurement, $\boldsymbol{H}$ is the state observation matrix, and $\boldsymbol{V}$ is the measurement noise covariance.

$$\boldsymbol{L_K} = \hat{\boldsymbol{P}}\boldsymbol{H}^{\boldsymbol{T}}\boldsymbol{V}^{-\boldsymbol{1}} \tag{A.2}$$

The measurement update of the state vector $\hat{\boldsymbol{\zeta}}$ is performed by using the Kalman gain, $\boldsymbol{L_K}$, the state estimate from the preceding time update, $\bar{\boldsymbol{\zeta}}$, the current measurement $\boldsymbol{z}$, and the state observation matrix $\boldsymbol{H}$ as shown by Equation A.3.

$$\hat{\boldsymbol{\zeta}} = \bar{\boldsymbol{\zeta}} + \boldsymbol{L_K}(\boldsymbol{z} - \boldsymbol{H}\bar{\boldsymbol{\zeta}}) \tag{A.3}$$

During the time update step there is no measurement, therefore the state is estimated based on the state transition matrix $\boldsymbol{\Phi}$ and the state value from the preceding measurement update, as shown by Equation A.4. The covariance at the time update, $\bar{\boldsymbol{P}}$, is given by Equation A.5 where the constant matrix $\boldsymbol{\Gamma W \Gamma^T}$ is given by Equation A.7.

$$\bar{\boldsymbol{\zeta}} = \boldsymbol{\Phi}\hat{\boldsymbol{\zeta}} \tag{A.4}$$

$$\bar{\boldsymbol{P}} = \boldsymbol{\Phi}\hat{\boldsymbol{P}}\boldsymbol{\Phi^T} + \boldsymbol{\Gamma W \Gamma^T} \tag{A.5}$$

The values of the state transition matrix, $\boldsymbol{\Phi}$, are determined by taking the matrix exponential of $\boldsymbol{F T_S}$, where $\boldsymbol{F}$ is the system matrix, and $\boldsymbol{T_S}$ is the sampling period. The values of this matrix remain constant as they are a property of the physical system and the fixed sampling frequency (see Equation A.6).

$$\boldsymbol{\Phi} = \begin{bmatrix} 1.0 & 0.001 \\ 0.0 & 1.0 \end{bmatrix} \tag{A.6}$$

The $\boldsymbol{\Gamma W \Gamma^T}$ matrix propagates the effects of the process noise which factors into the covariance calculation during the time update. Its value is constant and is found using the process covariance $\boldsymbol{W}$ and the input matrix $\boldsymbol{\Gamma}$ (see Equation A.7).

$$\boldsymbol{\Gamma W \Gamma^T} = \begin{bmatrix} 0.4 & 0.0 \\ 0.0 & 0.0 \end{bmatrix} \tag{A.7}$$

APPENDIX B

CONCEPTS

In an effort to cover a wide range of possible solutions to the task at hand, the concept section of this thesis presents concepts and ideas that although may be practical and highly effective, were not evaluated or developed beyond a conceptual level. The reasons vary though are mostly due to constraints in time and resources. These concepts represent further reaching ideas which may be considered more advanced than necessary for application in power tool safety. None the less, they are important to be presented since their potential is high and can serve as a starting point for further work.

B.1 Kerf Detection

This new concept of monitoring for a kickback safety hazard involves taking direct measurements at the root of the cause and thereby giving indications of an impending hazard, rather than other methods which look at indications that a kickback event has already begun occurring.

For the purposes of nomenclature, the beginning of the kickback is chosen as the point at which the work piece — initially having a positive feed velocity towards the blade — stops, and begins its backward movement, termed the kickback. This decision is arbitrary, but chosen so because it is a reference point that is easy to relate between the different sensors such as the encoder, accelerometer, as well as with any high speed video being captured. In fact, the complete kickback event has already begun at this point, because the reason for this flipping of the feed velocity is due to the initial stages of the kickback event itself.

With this new monitoring method, there is the ability to detect an impending kickback even before the beginning of the kickback as described in the preceding paragraph. In essence this allows not only for the detection of a kickback but also its prediction. There are no other known methods, in use or in concept that allow for this, therefore this is critical technology that would assist in the successful mitigation and prevention of potentially very hazardous kickback events.

The main idea of this concept is that it focuses on monitoring the cause of the kickback, rather than its effects. The effects of a kickback are the change of the work piece feed velocity, change in the tool blades angular velocity, as well as any generated vibrations throughout this process. It is critical to note that all of these begin to occur after the physical mechanics of the kickback are initiated, even though for reference purposes the beginning of the kickback is the point of reversal in the feed velocity. On the other hand, by monitoring the kerf (slot due to blade cut) width and position, there is the ability to *predict*, not just detect, when a kickback would occur; this is due to the way a kickback is induced.

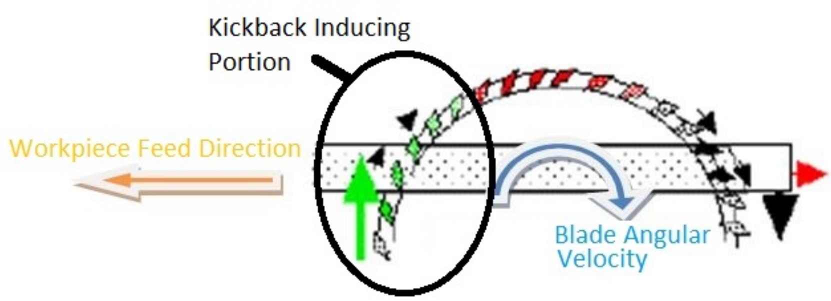

Figure B.1. Influence of blade areas on kickback

In the most general sense, a kickback is induced whenever there is a significant interaction between the blade and the teeth at the back of the blade, in Figure B.1 this portion is circled and noted. The issue is that, if for any reason the kerf closes up or becomes misaligned from being parallel to the blade, friction will being to build up and since the velocity vector of the teeth at this location generally point in the vertical direction, then the work piece will be lifted off the work table. In itself this is not a critical problem, but once the work piece is off the table, it will begin to make contact with the teeth at the top of the blade. At this point the main issue arises; the velocity vector of the teeth at the top is directed opposite to the feed direction.

Depending on the amount of binding and friction that is developed, there can and usually is a rapid and significant transfer of energy from the blade to the work piece, giving it velocity opposite the feed direction, which builds up abruptly in a manner of 100 to 200 milliseconds.

With other types of detection methods, there would be a need for this process to start before any issues can be detected, however with the kerf monitoring concept the issue can be detected before there is liftoff of the work piece from the work table, and long before there is contact with the teeth at the top which contribute most of the velocity of the kick back.

Another positive outcome of this concept is that it has the ability to predict kickback due to both of the identified modes of kickback induction, closing of the kerf and shifting of the kerf. Both of these modes lead to interaction of the rear of the blade and the work piece and result in the same final outcome. For the sake of clarity, shifting of the kerf essentially is equivalent to closing and pinching of the blade, except that it occurs only on one side of the blade.

With this method, there is a significant advantage in that an issue will be detected much earlier, and therefore allow much more time for any mitigation methods to be applied. Experimentation has shown that mitigating or preventing the kickback by stopping the blade requires the transfer or absorption of a high amount of momentum, and therefore every additional milliseconds gained from the detection phase allows for a more practical and effective mitigation strategy.

The operation of this method is quite simple as illustrated with the flow chart in Figure B.2; it requires only a sensor mounted in an appropriate location (multiple locations possible) such that there is a clear view of the kerf left behind the blade. Depending on the blade installed, a range on the allowable kerf width can be deter-

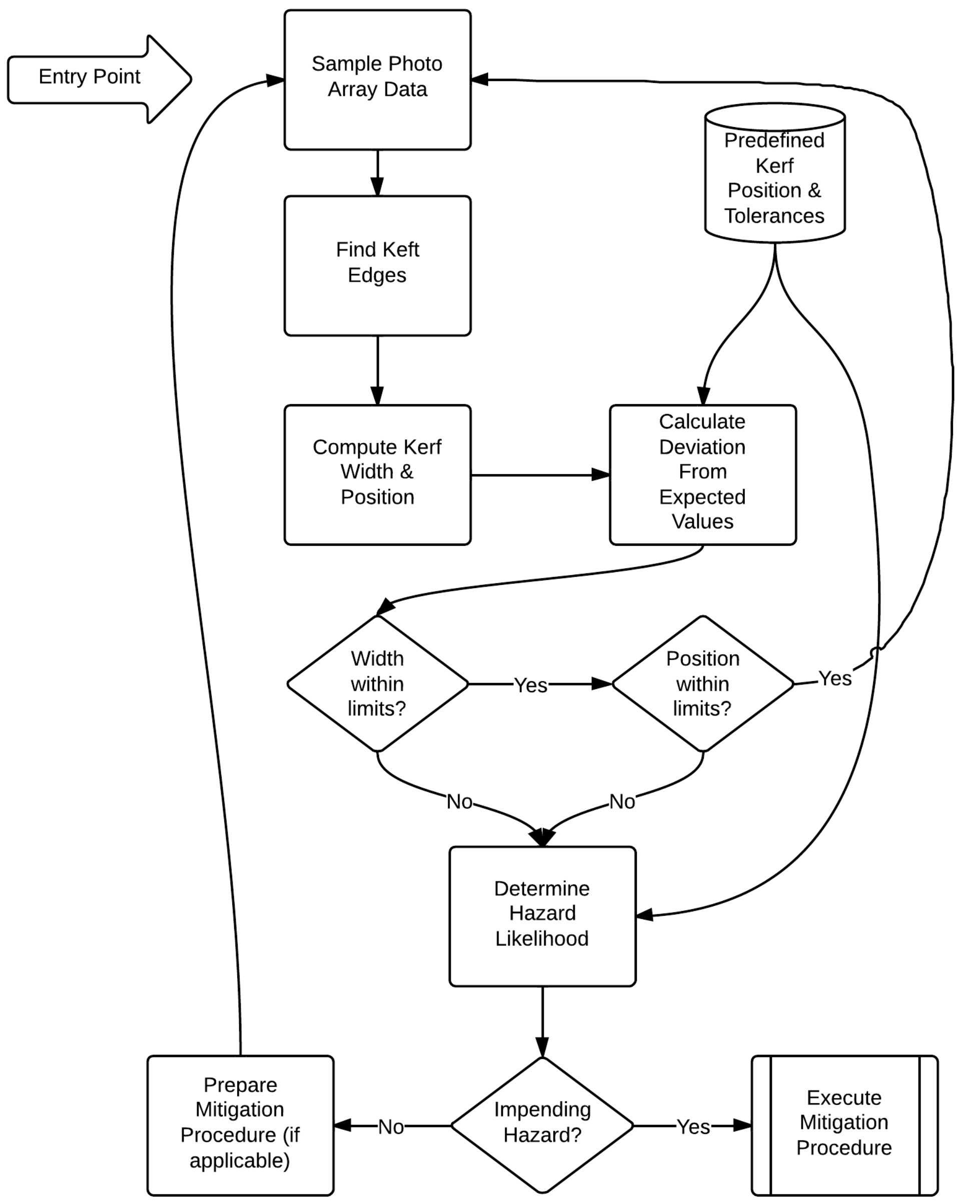

Figure B.2. Flow chart of the kerf based evaluation process)

mined such that there is allowance for some kerf width changes but not so much as to actually cause any type of kickback issue. This would be necessary to avoid false positives as the kerf varies continuously to some degree. The same thought can be applied to the shifting of the kerf, where an acceptable range of kerf edge positions can be determined. There is also the ability to set up the system such that it can automatically calibrate to the installed blade without any additional interaction. This could be done by using sensor reading from the point of first contact with the kerf (kerf at leading edge of the work piece) as a reference for the allowable range, rather than having predefined ranges.

The nature of this concept allows for a wide choice of implementation options, the only strict requirement is that the placement of any sensors allows for a clear view of the kerf or slot left by the cutting blade.

The main sensing task would be to identify the edges of the kerf in the work piece and to determine the distance between the two edges. In terms of sensing, there are two major requirements on the sensor used; one is the sampling rate and the other the resolution of the measurements. Neither of these is absolute, and would depend on the requirements of the entire system. The sampling rate of the sensors would highly depend on the performance of the mitigation method used, for a quick mitigation method the sampling can occur much slower since there is a greater window of detection. The measurement resolution on the other hand would need to be good enough to allow for detection of small changes in the kerf width, and the requirements will also be dictated by the overall system requirements. A lower resolution system can be used at the expense that small changes will not be detected and thus a larger kerf width change would need to occur before it is noticed. Keeping in perspective that the overall kerf width is around 2-3 millimeters, there is a limit on the minimum resolution that can be used.

Figure B.3 shows one of many possible embodiments where the sensor is mounted onto the upper guard (above the saws table) and faces the kerf of the exiting work piece.

Different methods of sensing are applicable in this case. Although direct com-

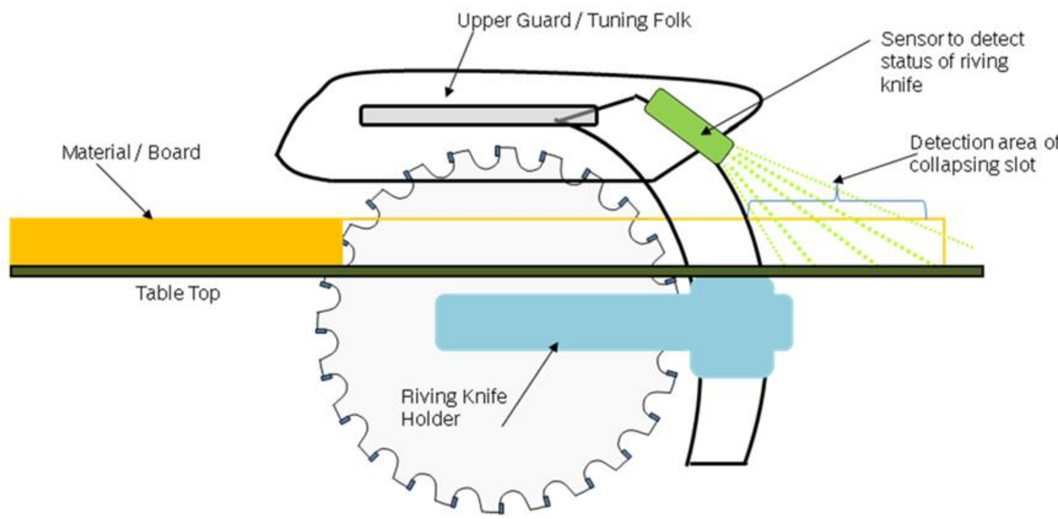

Figure B.3. Possible embodiment of Kerf sensing

mercial sensing solutions exist, they are by no means the only way nor the best way. The only need in this method is to be able to detect the edges of the kerf, and extract the distance between the two edges. The following is a list of possible sensor embodiments:

- 2-D Laser Profile Sensor
- Imaging Sensor (black and white is sufficient)
- Linear Photo Diode (optical) Array (low resolution is ok with appropriate optics)

The use of a commercial sensor such as a 2-D laser profiler or a high speed imaging sensor is ideal in the application of this concept, however the cost of these sensors is a significant hurdle. A quote from Keyence on such a profile sensor is about \$17,000, at such a cost the entire concept becomes invalid. This high cost is mostly due to the high speed and high accuracy of the sensors.

Aside from these sensors there are alternative approaches. One of the most appealing and practical alternatives is to develop a sensor specifically for this purpose, where low cost, low precision, and low speed components are combined in such a way as to deliver the required characteristics.

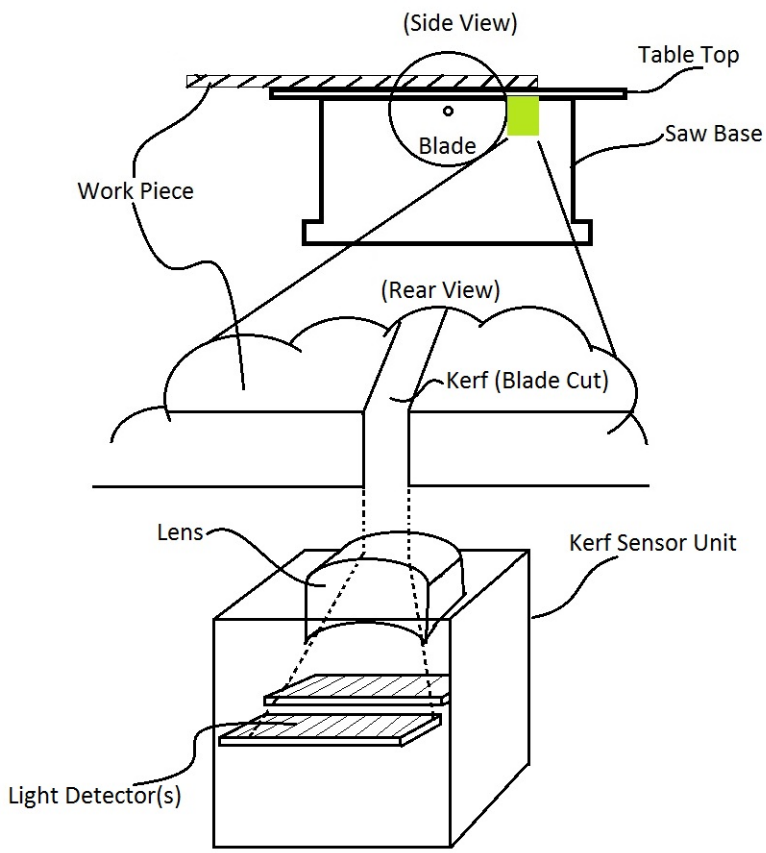

Figure B.4. Sketch of alternative cost effective sensor

A possible embodiment of such a sensor is sketched in Figure B.4. Here the idea is to use one or more low resolution linear optical arrays composed of light sensitive devices such as photo diodes or similar. Such arrays can be acquired for very low costs due to their low resolution, with available diode sensing element sizes of 1 mm and as small as 50 microns. In order for the sensor to have the proper resolution, a lens is placed in front of the array thereby magnifying the image of the kerf. This magnified image in effect reduces the required resolution of the sensing element, and is critical to substantially reducing the cost. For example, the MLX90255BC linear sensor array has a cost of \$7, can operate at a frequency of up to 800 kHz, and contains 128 active sensing diodes with each having a width of 66 microns. The overall length of the sensing array is 8.5 mm, which when coupled with an appropriate lens would deliver more than adequate resolution.

Although the sensor mentioned above has a sampling rate well within the requirements, there is the possibility to use multiple slower arrays aligned with the kerf, which can be sampled sequentially to provide multiples of the sampling rate of each individual sensor. This is indicated in Figure B.4.

As described, this sensor would be of a passive type, acquiring only the available light in the environment. To alleviate any potential issue due to a low light environment, a small light source such as an LED can be added to the sensor to provide constant illumination on the underside of the work piece at the location of the scanner. This addition essentially turns the sensor into an active light scanning type.

This concept has not been evaluated beyond a point of basic research and cross application comparison. Multiple other ways of implementing the sensing element, such as cheap bar-code scanners, are available as are many others. The potential for very early detection/prediction of an impending hazard is the most significant benefit offered, and further work most definitely needs to fully evaluate this effectiveness.

B.2 Neural Network State Prediction

Machine learning has found practical applications in many devices in the past decades. In recent times this technology has moved into the simplest of devices, such as the Nest Labs home thermostat [FRS$^+$13], to provide a level of performance that simply cannot be achieved through preprogrammed and predetermined processes.

This type of approach is necessary in applications where the targeted process is one that cannot be easily modeled or one where it is not consistent over time.

A machine learning approach can also be taken to improve the detection time of an active response technology system designed for kickback detection. Specifically, an artificial neural network (ANN) is applied such that it attempts to predict the state of the power tool at a future time, based on sensor input of the current state. A similar implementation for prediction of the remaining energy in a lead acid battery has been previously researched and shown to be effective [AGC09]. The purpose of the ANN is to predict the state of the tool at a later time; however the actual method of detecting the kickback is unchanged from that of the angular acceleration threshold method as presented in Section 2.3. In the angular acceleration threshold method, only the time derivative of the blade angular velocity is used in the detection of the kickback. For this particular concept, a simulation based on data gathered from the tool was evaluated to obtain an idea of the effectiveness. All training and performance testing has been done in MATLAB with the use of the Neural Network Toolbox. This software package was chosen due to convenience, however, any other Neural Network building and training software can be used and still obtain the same results. Equivalently the Neural Network may be built and trained without any specialized software, simply by implementing the desired algorithm.

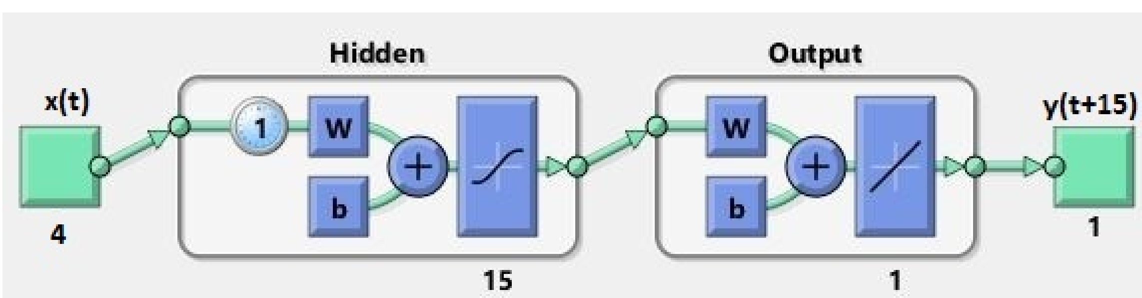

Figure B.5. Topology of the evaluated Neural Network

The topology of the network was kept as simple as possible, but still expected to deliver favorable results. This is shown in Figure B.5. The main reason for desiring a simple network is because this concept is developed with low-resource embedded hardware in mind.

Table B.1. NeuralNet inputs and outputs

Inputs(4) at x(t)	Output(1) at y(t+15)
Current Blade RPM Current X-Axis Acceleration Magnitude Current Y-Axis Acceleration Magnitude Current Z-Axis Acceleration Magnitude	Predicted Blade RPM - 15 samples into future

The training of the network consists of presenting it with four input signals and one output signal, as shown in Table B.1. The inputs, blade angular velocity and vibration data from the accelerometer in three orthogonal axes, are passed in at the current time step t, meaning there is no delay introduced. In this particular implementation the goal is to test the performance of the ANN with a prediction of 15 time steps, which at a sampling rate of 1 kHz equates to a prediction of 15 milliseconds into the future. To accomplish this in the training phase, the output data, or target data, presented to the ANN is shifted by 15 samples such that when input t is presented, the target output is that of $t + 15$. The output signal consists of only the blade angular velocity as it is the target of the prediction. The mean-squared-error (MSE) of the actual angular velocity and the predicted angular velocity is used to evaluate and propagate the training of the neural net in the proper direction until the improvement gradient from the MSE falls below some point. The signals presented to the network for training were collected during the kickback simulation trials as described in the previous chapters.

The results from this setup, with minor filtering (low pass) on the presented data have shown to be very promising. This is illustrated by the very low mean-

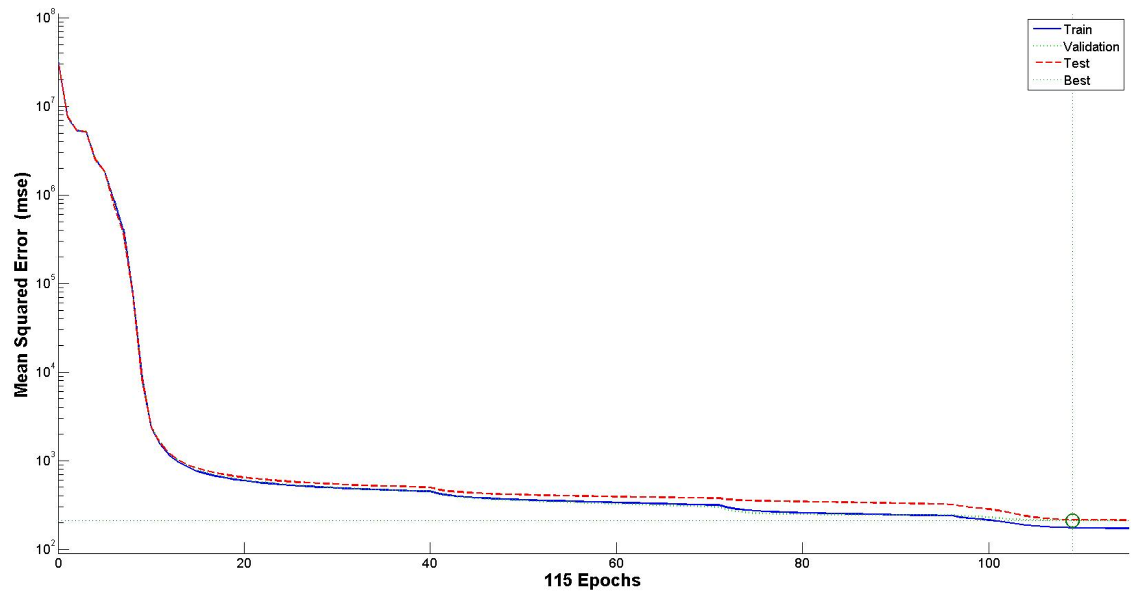

Figure B.6. Training performance mean-squared-error (MSE)

squared-error in Figure B.6, as well as in Figure B.7 showing the frequency and magnitude of the errors.

The resulting prediction of the tools angular velocity (in this case RPM) curve, is shown in Figure B.8. The most interesting result is how accurate the RPM curve is represented during the kickback event, although still containing significant error. This is not necessarily a negative outcome, as the ANN can be paired with a detection algorithm which not only looks for thresholds in predicted values, but can also be set up to trigger in events where the actual state of the tool deviates by a large amount from the predicted state from previous samples. This would be akin to suspecting that something abnormal is happening since the state is outside of the Neural Nets expectations.

In the proposed implementation, the ANN would be trained from many different sample trials. The result of this would be set of parameters describing the connections and weights between the neural functions. The parameters of the network can be installed in an embedded micro-controller such as in any of the other

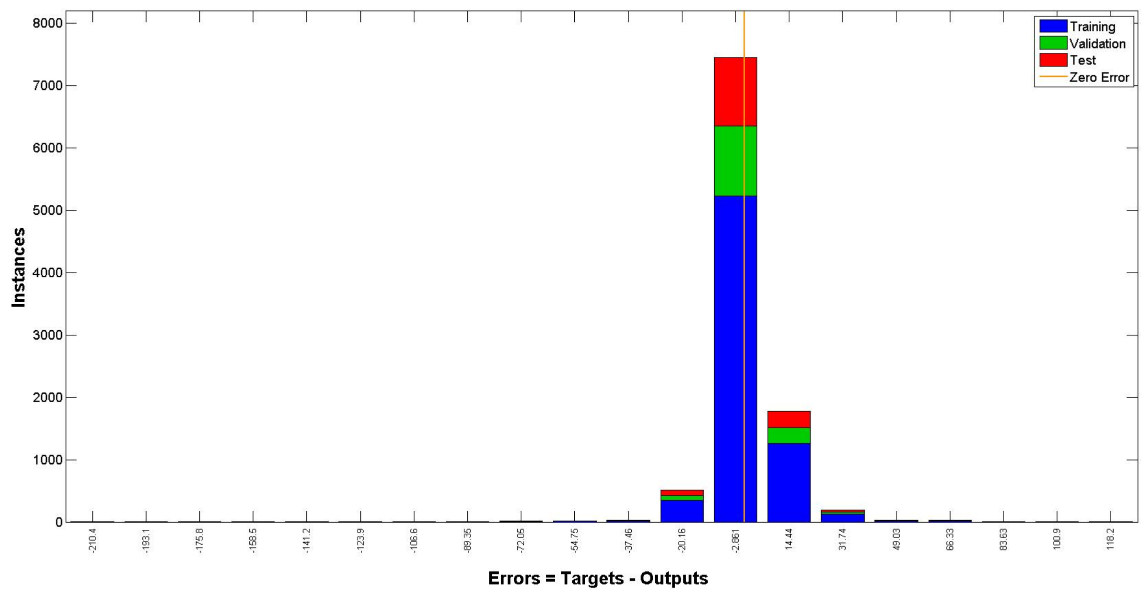

Figure B.7. Histogram of prediction errors

detection methods previously presented. An advantage of the ANN is that once trained, it is not computationally demanding, as it can be set up to involve algebraic calculations and matrix math, which has been shown to be effectively implemented in a micro-controller [AGC09, BG10]. At each sampling/evaluation period, the micro-controller would compare the predicted output of the ANN with that of the predefined threshold for a kickback event, and if the threshold is exceeded, the kickback event would be detected.

This brief evaluation is sufficient to show the potential of the method, however it is lacking in repeated trials to show the robustness and repeatability. Further work also needs to be done to find the optimal delay (or prediction time) that can be obtained by the ANN, as well as an optimal topology for the network. As the simple threshold method works quite well on its own, any additional time advantage that can be provided by the ANN will be highly advantageous in practical prevention/mitigation scenarios as this will allow more time for whichever actuation method is used. Additional time for actuation will have benefits in effectiveness, as well as

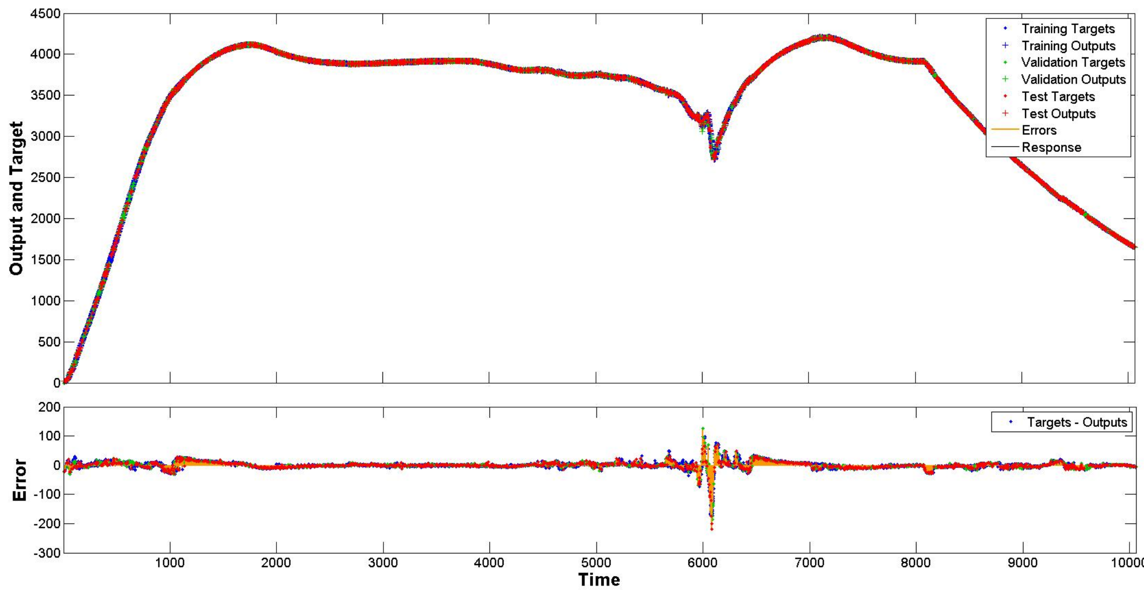

Figure B.8. Predicted time series curve of blade RPM

allow for a much simpler, cost effective, and overall practical mechanical system to be successfully implemented. It is also important to note that the chosen prediction interval, 15 time steps, has been selected for evaluation purposes but can be varied to any value that optimizes the results based on the system requirements and capacities.

BIBLIOGRAPHY

[AGC09] B. Akdemir, S. Gunes, and I. T. Comlekciler. Microcontroller compatible sealed lead acid battery remaining energy prediction using adaptive neural fuzzy inference system. In *Web Information Systems and Mining, 2009. WISM 2009. International Conference on*, pages 779–783, Nov 2009.

[ARM] ARM. *Cortex Microcontroller Software Interface Standard*, version 3.20 edition.

[Bel02] Charlie Belden. Kickback. Online Woodworking Blog, August 2002.

[BG10] R. Bayindir and A. Gorgun. Hardware implementation of a real-time neural network controller set for reactive power compensation systems. In *Machine Learning and Applications (ICMLA), 2010 Ninth International Conference on*, pages 699–703, Dec 2010.

[CP11] Sadeq R. Chowdhury and Caroleene Paul. Survey of injuries involving stationary saws. Technical report, U.S. Consumer Product Safety Commission, March 2011.

[FRS+13] A. Fadell, M. Rogers, E. Satterthwaite, I. Smith, D. Warren, J. Palmer, S. Honjo, G. Erickson, J. Dutra, and H. Fiennes. User-friendly, network connected learning thermostat and related systems and methods, April 25 2013. WO Patent App. PCT/US2012/030,084.

[Jas10] Jason. This is what table saw kickback looks like. Internet Blog, October 2010.

[MRM03] Natalie Marcy, George Rutherford, and Alberta Mills. Hazard screening report, power tools and workshop equipment. Technical report, U.S. Consumer Product Safety Commission, June 2003.

[Rob34] E.S. Robinson. *Handbook of General Experimental Psychology.* Clark University Press, Worcester, MA, 1934.

[SCB+12] E. J. Sharkey, M. Cassidy, J. Brady, M. D. Gilchrist, and N. NicDaeid. Investigation of the force associated with the formation of lacerations and skull fractures. *International Journal of Legal Medicine*, 126(6):835–844, 2012.

[SHV12] Toshak Singhal, Akshat Harit, and D. N. Vishwakarma. Kalman filter implementation on an accelerometer sensor data for three state estimation of a dynamic system. *international Journal of Research in Engineering and Technology (IJRET)*, 1(6):330–334, 2012.

[Smi11] Timothy P. Smith. Human factors evaluation of technology intended to address blade-contact injuries with table saws. Technical report, U.S. Consumer Product Safety Commission, July 2011.

[Spa12] Marc Spagnuolo. Woodworking injuries. Internet Article, May 2012.

[Wel80] A.T. Welford. *Reaction Times*, pages 73–128. Academic Press, New York, 1980.

[Win09] T. Winkler. Schutzsystem für werkzeugmaschinen protection system for machine tools, October 1 2009. DE Patent App. DE200,810,000,891.

[Win11a] T. Winkler. Emergency braking system for machine tools, March 3 2011. US Patent App. 12/806,140.

[Win11b] T. Winkler. Tool device i.e. saw device, for use in e.g. table circular saw, has two fastening parts, where one of parts is provided for form-fittingly attachment of tool and other part with respect to circumferential direction of output shaft, March 3 2011. DE Patent App. DE200,910,029,066.